Li, Mengheng; Mendieta-Muñoz, Ivan

Working Paper

Dynamic hysteresis effects

Working Paper, No. 2024-01

Provided in Cooperation with:
Department of Economics, The University of Utah, Salt Lake City

Suggested Citation: Li, Mengheng; Mendieta-Muñoz, Ivan (2024) : Dynamic hysteresis effects, Working Paper, No. 2024-01, The University of Utah, Department of Economics, Salt Lake City, UT

DEPARTMENT OF ECONOMICS WORKING PAPER SERIES

Dynamic hysteresis effects

Mengheng Li
Ivan Mendieta-Muñoz

Working Paper No: 2024-01

January 2024

University of Utah
Department of Economics
260 S. Central Campus Dr., GC. 4100
Tel: (801) 581-7481
Fax: (801) 585-5649
http://www.econ.utah.edu

Dynamic hysteresis effects*

Mengheng Li†

Ivan Mendieta-Muñoz‡

January 4, 2024

We study how the output gap affects potential output over time—*i.e.*, the dynamic hysteresis effect. To do so, we introduce novel unobserved components (UC) models that consider hysteresis as a sequence of lagged effects, thus separating the long-run recession-induced adverse effects from other trend-cycle interactions. The proposed models nest several existing UC models in the literature and accommodate two key characteristics of output dynamics: non-neutrality in the long-run and the time-to-build effect. Using Bayesian estimation methods, we find robust evidence supporting the presence of hysteresis effects after the 1970s, with the negative long-run effect of the Global Financial Crisis and the COVID-19 recessions robustly identified. Via Bayesian model averaging, we provide precise and intuitive output gap estimates that highlight the relationship between business cycle fluctuations and the decline in economic growth. Our findings indicate that output trend-cycle decompositions that do not consider hysteresis effects can alter stabilization policy trade-offs.

Keywords: hysteresis; time-to-build effect; trends and cycles; permanent and transitory shocks; state space models; unobserved components.

JEL Classification: C11; C32; E10; E32; O40.

*We are deeply grateful to Joshua Chan, James Morley and Adrian Pagan for valuable comments and suggestions. Any remaining errors are the responsibility of the authors.

†Senior Lecturer (Assistant Professor). University of Technology Sydney (UTS) Business School and Centre for Applied Macroeconomic Analysis (CAMA). Email: mengheng.li@uts.edu.au

‡Associate Professor. Department of Economics, University of Utah. Email: ivan.mendietamunoz@utah.edu

1 Introduction

The standard view presented by most introductory and intermediate-level macroeconomics textbooks is that cycles, driven by transitory or demand shocks, and trends, driven by permanent or supply shocks, exist as separate phenomena. The concept of hysteresis, however, allows for the possibility of studying the interactions between cycles and trends in a unified framework. If hysteresis effects are relevant, then cycles driven by demand shocks—especially those associated with large recessions—can have permanent effects on trends.

In this paper, we present novel models and methods aimed at estimating the evolution of hysteresis effects over time, which we call dynamic hysteresis effects. To do so, we modify the structure of unobserved components (UC) models by incorporating different timings that capture a rich set of dynamic interactions between trends and cycles in output. We call the proposed baseline model the hysteresis correlated unobserved components (HCUC) model, which allows us to disentangle the long-run adverse effects associated with recessions from other important effects that may also exist, such as time-to-build effects in the context of correlated unobserved components (CUC) models for output. Thus, the HCUC model is designed to capture two plausibly relevant characteristics of an economy: non-neutrality in the long-run by introducing dynamic hysteresis effects and time-to-build effects by introducing correlation between permanent and transitory innovations.

Using Bayesian estimation methods, we find two main empirical results for the US economy. First, recessions have affected negatively potential output growth since the early 1970s, so hysteresis effects have become more relevant to understand the dynamics of potential output growth since then. Second, compared to the CUC model, the HCUC model estimates a lower time-to-build effect, yields a more consistent and intuitive output gap estimate, and improves the model fit of real GDP according to Bayesian model comparison methods. These results are robust to several extensions of the baseline model also developed in the current article, specifically, HCUC models that: (i) separate the effects of recessions and expansions; (ii) consider a real-time recession indicator; (iii) introduce nonlinear effects via Markov regime switching; (iv) consider a multivariate framework; and (v) contain alternative priors. Overall, the empirical findings emphasize the increasing relevance of studying cyclical long-run non-neutral effects and that conceptualizing the hysteresis effect and the time-to-build effect as two different economic phenomena improves our understanding of the interactions between

trends and cycles.

Our contribution is mainly related to two bodies of literature. First, notwithstanding its conceptual importance, the empirical evidence in favor or against of hysteresis effects is still open to debate (see also Blanchard, 2018, for example). While Cerra and Saxena (2008) found that deep recessions permanently reduced GDP in a sample of 190 countries, Teulings and Zubanov (2014) and Bakas and Mendieta-Muñoz (2020) reported different results when alternative specifications and estimators are used. Ball (2009) argued that the natural rate of unemployment is affected by aggregate demand in 20 developed countries, so hysteresis effects are important; however, his estimation framework does not allow for a clear-cut separation between permanent and highly persistent effects. Ball (2014) found evidence of hysteresis effects in output in 23 countries associated with the Great Recession; but Eo and Morley (2022) reported that the Great Recession generated a large, persistent negative output gap rather than any hysteresis effects in the US economy. Blanchard et al. (2015) report some evidence of hysteresis effects for a sample of 23 advanced economies: (i) approximately two-thirds of recessions have been followed by lower output trends; (ii) in 50 percent of those cases output growth rates also fell; and (iii) in 63 percent (20 percent) of those cases recessions that are most likely associated with demand shocks have been followed by lower output trends (lower output growth rates).[1] Recent results using SVAR models for the US economy also provide mixed evidence. Furlanetto et al. (2021) and Maffei-Faccioli (2021) found support for the relevance of hysteresis effects by combining long-run zero and short-run sign restrictions and using long-run sign restrictions, respectively; whereas Benatti and Lubik (2022) employ a combination of long-run zero restrictions and both short- and long-run sign restrictions, finding that hysteresis effects: (i) are virtually absent for samples excluding the Great Recession of 2007-9; (ii) only appeared when including the period following the collapse of Lehman Brothers; and (iii) possess a high probability of detection even when the data-generating process (DGP) features none by construction.

Second, structural time series analysis, in general, and the CUC model, in particular, represents a simple but notable alternative for studying the existence of hysteresis effects since it allows researchers to explicitly model the interactions between permanent and transitory

[1] According to Blanchard et al. (2015), demand shocks are those associated with intentional disinflations, which happened mostly in the 1980s and early 1990s.

shocks.[2] Although different contributions have shown the relevance of these interactions by considering both univariate and multivariate CUC models for output, the estimation and interpretation of hysteresis effects via CUC models also remains unclear.[3] To sum up, as discussed by Morley (2007) and Weber (2011), the CUC model does not posses a structural interpretation. In other words, if permanent and transitory shocks are correlated, then the reduced-form permanent and transitory shocks represent linear combinations of the structural trend and cycle shocks.[4] Li and Mendieta-Muñoz (2022) have recently shown that every CUC model has a structural representation, so that the magnitude and direction of the possible interactions among different unobserved components can be identified via the respective structural CUC model. Nevertheless, the identification of possible hysteresis effects in this context depends on the assumption that changes in the reduced-form covariance matrix in a CUC model are derived from heteroskedasticity in its structural representation. The latter is statistically relevant; however, it may not be a necessary or sufficient condition for the existence of hysteresis since the extant theoretical literature has not referred to this possibility when discussing the relevant channels in which hysteresis effects may arise.[5]

The current research contributes to the two aforementioned bodies of literature as follows. With respect to the first, since our work develops UC models that explicitly consider different timings to separate the hysteresis and time-to-build effects, our approach differs from the use of SVAR models by using structural time series analysis, which addresses the concern of Fisher et al. (2016) that differentiating permanent and transitory shocks in SVAR models is essentially a subjective decision. Two further examples that illustrate this point can be provided. Firstly, as discussed by Keating (2013a,b), structural shocks can possess different interpretations if demand shocks are partially permanent in the Blanchard and Quah (1989) decomposition. Secondly, also related to the latter, the evidence found by Cover et al. (2006) and Bashar (2011) is that demand

[2] If permanent and transitory shocks are assumed to be independent, then the CUC model corresponds to the standard UC model (Harvey and Shephard, 1993; Durbin and Koopman, 2012).

[3] Univariate CUC models such as Morley et al. (2003) and Dungey et al. (2015) have been proposed for the analysis of the dynamics of US output; whereas multivariate CUC models that show the presence of both within-series and cross-series correlations between permanent and transitory shocks include Basistha (2007)—who studied output and inflation, Sinclair (2009)—who studied output and unemployment, and Mitra and Sinclair (2012)—who studied output across the G-7 countries.

[4] See also Proietti (2006) and González-Astudillo and Roberts (2022), who point out that several subtleties and interpretative issues arise from trend-cycle decompositions with correlated components.

[5] Different economic theories that allow for various types of interactions between trends and cycles have been proposed by several bodies of literature. Keating (2013a), Mendieta-Muñoz (2017), Garga and Singh (2021), Fatás and Singh (2022), Galí (2022) and Cerra et al. (2023) provide extensive literature reviews. Indeed, none of these theories has explicitly associated the presence of hysteresis effects with the heterogeneity of variance.

and supply shocks can be highly correlated, so that permanent changes in the economy associated with the supply side are not independent of temporary changes associated with demand in the G-7 countries.[6] Hence, although we remain agnostic about the specific nature of the shocks that affect the permanent and transitory components of output, we are to able to provide a direct answer to a simple conceptualization of hysteresis: does the statistical evidence support the view that large negative output gaps affect potential output growth over time?[7]

Regarding the second body of literature, since the empirical findings support the proposed HCUC models by showing that the latter yield more consistent and intuitive output gap estimates and improve the model fit of GDP in the US compared to CUC models, our research stresses that it is beneficial to explicitly consider the hysteresis effect and the time-to-build effect as two alternative sources of interaction between trends and cycles in output. In other words, it is necessary to conceptualize the possible permanent effects derived from recessions (hysteresis) and those related to positive supply shocks (time-to-build) as two separate phenomena. In this sense, the proposed models and methods extend our understanding of the interactions between cycles and trends by enriching the structure of UC models.

Besides this introduction, the rest of the paper comprises the following sections. Section 2 describes the CUC models with hysteresis effects and the estimation approaches. Section 3 summarizes the main empirical findings. Section 4 discusses the main results focusing on the relevant policy implications. Finally, the main conclusions are presented in section 5.

2 The correlated unobserved components model with dynamic hysteresis effects

We present the baseline model that extends the CUC model by introducing non-neutrality in the long-run via dynamic hysteresis effects, followed by the identification conditions and the Bayesian estimation procedure. Finally, we discuss model extensions that deal with some limitations of the baseline specification.

[6] Interestingly, however, supply shocks do not seem to be sensitive to demand shocks in other developing countries, such as Mexico (Mendieta-Muñoz, 2018).

[7] Section 2.4 in the paper clarifies this point further.

2.1 Model specification

Let y_t denote the logarithm of the US real GDP and $t = 1, ..., T$. We propose the following HCUC model, that is, a correlated unobserved components model with dynamic hysteresis effects:

$$y_t = \tau_t + c_t, \tag{1}$$

$$\Delta\tau_t = \gamma_t + \eta_t, \tag{2}$$

$$\phi(L)c_t = \epsilon_t, \tag{3}$$

$$\begin{pmatrix} \eta_t \\ \epsilon_t \end{pmatrix} \sim N(\mathbf{0}, \mathbf{\Sigma}), \quad \mathbf{\Sigma} = \begin{bmatrix} \sigma_\eta^2 & \rho\sigma_\eta\sigma_\epsilon \\ \rho\sigma_\eta\sigma_\epsilon & \sigma_\epsilon^2 \end{bmatrix}, \tag{4}$$

$$\gamma_t = \boldsymbol{z}_t(\mu_1, \mu_2, \boldsymbol{\beta}')', \tag{5}$$

$$\boldsymbol{z}_t = \left(\mathbb{1}_{\{t<t_0\}}, \mathbb{1}_{\{t\geq t_0\}}, \mathbb{1}_{\{t-1\in R\}}c_{t-1}, ..., \mathbb{1}_{\{t-k\in R\}}c_{t-j}\right), \tag{6}$$

where τ_t is the non-stationary permanent component of y_t, and c_t is the stationary transitory component of y_t. The components τ_t and c_t can be called the trend (or potential output) and the cycle (or output gap) of y_t, respectively.[8] Also, L is the lag operator, $\Delta = 1 - L$ is the difference operator, $\phi(L) = 1 - \sum_{i=1}^{p} \phi_i L^i$ is an order-p autoregressive (AR(p)) polynomial, and $\mathbf{0}$ is a zero matrix or vector of conformable size unless otherwise specified. The output gap dynamics and error structure shown in equations (3) and (4), respectively, follow the usual specifications of the CUC models studied by Morley et al. (2003) and Sinclair (2009). We follow Grant and Chan (2017) and initialize the model by considering τ_0 as a parameter and $c_h = 0$ for $h \leq 0$.

The main innovation of the above HCUC model is the incorporation of past cycles in the dynamics of potential output τ_t via the cycle effect on the potential growth rate γ_t. This is shown in equations (5) and (6), where τ_t is a random walk with a time-varying drift γ_t, given the predetermined time-variant row vector $\boldsymbol{z}_t$. The coefficient vector in equation (5) consists of two parts. First, μ_1 and μ_2 are the mean potential growth rates before and after a structural break occurring at t_0, respectively. Second, $\boldsymbol{\beta} = (\beta_1, ..., \beta_k)'$ collects the hysteresis coefficients,

[8] As Harvey and Shephard (1993) pointed out, if τ_t and c_t are assumed to evolve independently, the model is structural because only trend shocks affect y_t permanently; while the effect of cycle shocks vanishes in the long-run due to the stationarity condition. In this sense, if y_t corresponds to the log real GDP and if we assume long-run neutrality, it is possible to say that the estimated τ_t and c_t are driven by supply and demand shocks, respectively, and that the trend (the cycle) corresponds to potential output (output gap). In this paper we use the terms trend and potential output (cycle and output gap) interchangeably.

which include the past cycles affecting the permanent component of output. In equation (6), $\mathbb{1}_A$ is an indicator function that equals 1 if the respective condition in A is satisfied and 0 otherwise.

We consider a one-time break in the dynamics of γ_t in order to capture the change in potential output growth. There is ample evidence suggesting a secular decline in the post-war US GDP growth rate due to supply-side factors, such as slower productivity growth and falling labor force participation—see *e.g.* Gordon (2015), Fernald et al. (2017), Antolin-Diaz et al. (2017), Grant and Chan (2017), Li and Mendieta-Muñoz (2020), and Hasenzagl et al. (2022). Although it is possible to consider a gradually changing drift, Grant and Chan (2017) found overwhelming evidence in favor of a model with only one break over models with multiple breaks or gradual changes via comprehensive Bayesian model comparisons. Likewise, treating the drift component as an extra stochastic process introduces an additional innovation that unnecessarily complicates the model's identification. Hence, in the HCUC model we attribute the supply-driven permanent drop in potential output growth to the estimated difference $\mu_2 - \mu_1$.

Besides the declining potential output growth rate, $\boldsymbol{z}_t$ models dynamic hysteresis effects via $\boldsymbol{\beta}$. In equation (6), R collects time indices for when past cycles affect the potential output. We clarify three points. First, if $\boldsymbol{\beta} = \mathbf{0}$, the effect of c_t on y_t is transitory due to the stationarity condition. On the other hand, if $\boldsymbol{\beta} \neq \mathbf{0}$, such fluctuations affect τ_t and, thus, y_t permanently. The latter is the hysteresis effect, which would imply that the assumption of long-run neutrality no longer holds (Cerra et al., 2023).[9]

Second, the choice of R is important. Our baseline HCUC model shown in equations (1) through (6) considers that $\boldsymbol{z}_t$ is a function of a predetermined R. When discussing hysteresis effects, macroeconomists often refer to the adverse effect of large negative demand shocks associated with recessions on long-run growth rates (see, *e.g.*, Cerra and Saxena, 2008 and Ball, 2014). Therefore, we follow the standard approach and specify R to be an extended recession set that covers NBER-dated recessions and two extra quarters preceding and succeeding each recession. In the online appendix, we show that our results are robust to R covering more quarters (four and eight) after each NBER-dated recession.

Consider a setting where a recession occurs in period one and lasts four periods. We are

[9]Notice that, similar to Blanchard et al. (2015), we restrict c_t to have only lagged effects on γ_t. After all, the original Greek word for "hysteresis" means "lagging behind". Moreover, including the contemporaneous effect of c_t in (5) creates a tension between the actual hysteresis effect and the effect derived from the innovation correlation ρ, which we explore in section 3.3.

Table 1: An example of dynamic hysteresis effects

Period t	1	2	3	4	5	6	7	8	9	10
Recession	✓	✓	✓	✓	✓	×	×	×	×	×
	Effect of past cycles									
c_{t-1}	0	$\beta_1 c_1$	$\beta_1 c_2$	$\beta_1 c_3$	$\beta_1 c_4$	$\beta_1 c_5$	0	0	0	0
c_{t-2}	0	0	$\beta_2 c_1$	$\beta_2 c_2$	$\beta_2 c_3$	$\beta_2 c_4$	$\beta_2 c_5$	0	0	0
c_{t-3}	0	0	0	$\beta_3 c_1$	$\beta_3 c_2$	$\beta_3 c_3$	$\beta_3 c_4$	$\beta_3 c_5$	0	0
c_{t-4}	0	0	0	0	$\beta_4 c_1$	$\beta_4 c_2$	$\beta_4 c_3$	$\beta_4 c_4$	$\beta_4 c_5$	0
	Total effect									
HE_t	0	$\beta_1 c_1$	$\sum_1^2 \beta_i c_{3-i}$	$\sum_1^3 \beta_i c_{4-i}$	$\sum_1^4 \beta_i c_{5-i}$	$\sum_1^4 \beta_i c_{5-i}$	$\sum_1^3 \beta_i c_{7-i}$	$\sum_1^2 \beta_i c_{8-i}$	$\beta_4 c_5$	0

Notes: The dynamic hysteresis effect at time t equals the total effect of past cycles multiplied by their corresponding coefficients. In this example, we assume that $k = 4$.

interested in the dynamic hysteresis effect defined as:

$$HE_t = \sum_{i=1}^{k} \mathbb{1}_{\{t-i \in R\}} \beta_i c_{t-i}, \tag{7}$$

where $k = 4$. Table 1 illustrates the dynamic hysteresis effects in the HCUC model derived from such a recession from $t = 1$ through $t = 10$. Two interesting features emerge in this setting: (i) a full-scale hysteresis effect takes place shortly after the economy enters a recession and does not fully die out until some periods after the recession is over; and (ii) because HE_t corresponds to the sum of past cycle effects, the estimated hysteresis effects can adopt different dynamics—such as "fade-in", "fade-out", abrupt changes, or even oscillations—depending on the values of the c_{t-i}'s and β_i's coefficients. To summarize, we consider that HE_t possesses (deterministic) regime switching dynamics. With the recession indicators $\mathbb{1}_{\{t-i \in R\}}$, $i = 1, ..., k$, HE_t can adopt 2^k regimes, extending the space of possible hysteresis effects in the model.

Third, the correlation coefficient ρ in (4) allows the trend and the cycle shocks to be correlated. This is a key specification in many existing CUC models that does not preclude the possibility that demand shocks are non-neutral in the long-run; however, as mentioned above, this implies that the trend shock η_t and the cycle shock ϵ_t are no longer structural shocks.[10] In CUC models for GDP, Morley et al. (2003), Basistha (2007), Sinclair (2009), and Li and Mendieta-Muñoz (2022) document a large negative correlation coefficient of approximately -0.9. Morley et al. (2003) interpret this as a "time-to-build effect": a large positive permanent shock, *e.g.* due to

[10] Namely, it is not possible to separate permanent (supply) and transitory (demand) shocks without further assumptions (Keating, 2013b; Li and Mendieta-Muñoz, 2022).

technological progress, makes the output gap temporarily below potential until it catches up.

Therefore, besides including the contemporaneous correlation of shocks via ρ, in the HCUC model we also allow for long-run non-neutrality by explicitly incorporating dynamic hysteresis as lagged effects, as defined in equation (7). Due to the different timing assumed for the two effects, we are able to disentangle hysteresis effects from the possible time-to-build effects.

In sum, the baseline HCUC model is able to simultaneously study relevant characteristics of output dynamics: (i) the secular decline in potential output growth; (ii) the time-to-build effect; and (iii) the dynamic hysteresis effects. In this sense, the HCUC model nests the UC and the CUC models as special cases. The UC model imposes no hysteresis or time-to-build effects, *i.e.*, $\boldsymbol{\beta} = \mathbf{0}$ and $\rho = 0$. The CUC model allows for the time-to-build effect, but no hysteresis effects, *i.e.*, $\boldsymbol{\beta} = \mathbf{0}$ and $\rho \neq 0$. The HCUC model also nests an UC model with dynamic hysteresis effects (HUC model), which allows only for hysteresis effects with $\boldsymbol{\beta} \neq \mathbf{0}$ and $\rho = 0$.[11]

2.2 Identification

There are $p + k + 3$ parameters in the proposed baseline HCUC model: p AR parameters, k hysteresis parameters, and 3 variance-covariance coefficients. This section discusses the order and rank conditions for identification.

2.2.1 Necessary order condition

Consider a model with $R = \{1, ..., T\}$, *i.e.*, hysteresis effects are always present. Define $\beta(L) = \beta_1 + \beta_2 L + ... + \beta_k L^{k-1}$, such that HE_t in (7) equals $\beta(L)c_{t-1}$. We can rewrite (2) as

$$\begin{aligned} \phi(L)\Delta y_t &= \phi(L)(\mu + \eta_t + \beta(L)c_{t-1}) + \Delta\epsilon_t \\ &= \phi(1)\mu + \phi(L)\eta_t + \Delta\epsilon_t + \beta(L)\epsilon_{t-1} \\ &= c + \theta(L)u_t = c + m_t, \end{aligned} \tag{8}$$

where $\theta(L) = 1 + \theta_1 L + ... + \theta_q L^q$. Therefore, the reduced-form of y_t has an ARIMA$(p, 1, q)$ representation. The moving average (MA) part $m_t = \theta(L)u_t$ in (8) has order $q = \max(p, k)$. The autocovariances of m_t give $1 + q$ reduced-form parameters. With $3 + k$ parameters in $\boldsymbol{\Sigma}$ and $\boldsymbol{\beta}$, the order condition is satisfied only if $q \geq 2 + k$. Together with $q = \max(p, k)$, this implies

[11] Section 3.4 carries out the relevant comparisons among the model's variants.

that $p = q$. Therefore, the reduced-form ARIMA representation of y_t must have order $(p, 1, p)$ for identification and satisfies the necessary order condition $p \geq 2 + k$.

For example, in an HCUC model where only c_{t-1} enters the equation for τ_t, or $k = 1$, exact identification requires the cycle to be an AR(3) process. In a model with c_{t-1} and c_{t-4} entering the τ_t equation, or $k = 4$, identification requires the cycle to be at least an AR(6) process.

Regarding the growth rate of US real GDP, Δy_t is best fitted by an AR(3) or AR(4) process, so $p \geq 2 + k$ may be too restrictive. In a model where hysteresis effects are always present, this is indeed true. However, in an economy where expansions and recessions occur over time, the relevant order condition is almost surely satisfied. To see this, we first note that if $k = 0$, $p = 2$ or an AR(2) cycle suffices to identify $\boldsymbol{\Sigma}$ (see also Weber, 2011 and Li and Mendieta-Muñoz, 2022). If $\boldsymbol{\Sigma}$ is identified, then there are at least $1 + k$ non-zero autocovariances of m_t that are functions of k unknown β_i's. From a method of moments approach, the first three autocovariances of m_t during expansions (*i.e.*, $\boldsymbol{\beta} = \mathbf{0}$) provide enough information for $\boldsymbol{\Sigma}$. Given an identified $\boldsymbol{\Sigma}$, the last k autocovariances during recessions provide enough information to identify $\boldsymbol{\beta}$.

2.2.2 Sufficient rank condition

From the reduced-form representation shown in equation (8), the AR coefficients are identified. Assuming that there are no common roots to $\phi(L)$ and $\theta(L)$ (*i.e.*, there exists no value z^* such that $\phi(z^*) = \theta(z^*) = 0$), the AR part in (8) can be separated from the MA part such that we can consider the reduced-form AR coefficients as given (Hotta, 1989).

The difficulty in deriving primitive conditions that guarantee the identification of $\boldsymbol{\Sigma}$ and $\boldsymbol{\beta}$ comes from the nonlinear mapping from autocovariances of m_t to $\boldsymbol{\Sigma}$ and $\boldsymbol{\beta}$. There exists no analytical solution to this mapping. To see this, consider $p = 3$ and $k = 1$, which corresponds to the simplest model that satisfies the order condition when hysteresis effects are always present.[12] Let us omit the subscript of β_1 and define $b = \beta - 1$. The MA component in (8) is given by

$$m_t = \theta(L)u_t = \eta_t - \phi_1\eta_{t-1} - \phi_2\eta_{t-2} - \phi_3\eta_{t-3} + \epsilon_t + b\epsilon_{t-1}.$$

Let the autocovariances be defined by $g_h = E(m_t m_{t-h}) = \sum_{i=0}^{3-h} \theta_i\theta_{i+h}\sigma_u^2$, $h = 1, 2, ...$, such that

[12] The discussion below can be easily extended to models with $k > 1$. We omit such extensions because these merely involve a more elaborate mathematical notation.

$g_h = 0$ for $h > 3$. Let $\rho = \sigma_{\eta\epsilon}/(\sigma_\eta \sigma_\epsilon)$. It is possible to verify that:

$$\begin{pmatrix} g_0 \\ g_1 \\ g_2 \end{pmatrix} = \begin{bmatrix} 1+\phi_1^2+\phi_2^2+\phi_3^2 & 1-\phi_1 b & 1+b^2 \\ -\phi_1+\phi_1\phi_2+\phi_2\phi_3 & -\phi_1-\phi_2 b & b \\ -\phi_2+\phi_2\phi_3 & -\phi_2-\phi_3 b & 0 \end{bmatrix} \begin{pmatrix} \sigma_\eta^2 \\ \sigma_{\eta\epsilon} \\ \sigma_\epsilon^2 \end{pmatrix}, \tag{9}$$

$$g_3 = -\phi_3\sigma_\eta^2 - \phi_3 b \sigma_{\eta\epsilon}.$$

In principle, we can solve for the four unknowns depicted above. However, b appears in (9) nonlinearly, which creates multiplicity issues. The latter can be largely mitigated if we consider the problem recursively: given b, we can solve for $\text{vech}(\boldsymbol{\Sigma}) = (\sigma_\eta^2, \sigma_{\eta\epsilon}, \sigma_\epsilon^2)'$; and, given the latter, b can be identified from the last equation in (9).

Let the first equation in (9) be written as $\boldsymbol{g} = \boldsymbol{A}(b)\text{vech}(\boldsymbol{\Sigma})$. The task is then to check if $\boldsymbol{A}(b)$ has full rank. Let $A_{ij}(b)$ denote the (i,j)-th element of $\boldsymbol{A}(b)$. The matrix $\boldsymbol{A}(b)$ is rank-deficient if there exists $\boldsymbol{\alpha} = (\alpha_1, \alpha_2)' \neq \boldsymbol{0}$ such that $\boldsymbol{A}^*(b)\boldsymbol{\alpha} = \boldsymbol{0}$, where

$$\boldsymbol{A}^* = \begin{bmatrix} A_{11} - \frac{1+b^2}{b} A_{21} & A_{31} \\ A_{12}(b) - \frac{1+b^2}{b} A_{22}(b) & A_{32}(b) \end{bmatrix}.$$

The factor $-(1+b^2)/b$ is determined by noticing that $A_{33} = 0$, so that the only way to make $\alpha_1\big((A_{13}(b) + aA_{23}(b)\big) = 0$ is to set $a = -(1+b^2)/b$. Clearly, $\boldsymbol{A}(b)$ is rank-deficient only if $\boldsymbol{A}^*(b)$ is rank-deficient; but this is almost surely impossible because $\det[\boldsymbol{A}^*(b)] = 0$ implies that b must adopt some disjoint numbers, which are zero probability events. For this example ($k = 1$), it can be easily verified that $\det[\boldsymbol{A}^*(b)]$ yields a cubic polynomial in b that has at most 3 disjoint roots. Therefore, under the order condition $p = 2 + k$, the rank condition is also satisfied.

This discussion clarifies that, if the HCUC model distinguishes recessions from expansions, then the rank condition is automatically satisfied. From a method of moments approach, during expansions, $b = -1$ and $\text{vech}(\boldsymbol{\Sigma})$ is uniquely identified from $\boldsymbol{g}$, as in the first equation of (9) (that is, the first three autocovariances of the reduced-form representation). Therefore, $\boldsymbol{\beta}$ is uniquely identified from the last k autocovariances, as in the last equation of (9).

Lastly, Basistha (2007) and Li and Mendieta-Muñoz (2022), among others, showed that a CUC model tends to push ρ towards -1 even when the true DGP has zero trend-cycle correlation $\rho = 0$, a feature also noted by Morley et al. (2003). In the online appendix, we conducted a Monte

Carlo study with $\rho = 0$ in the DGP and find that the proposed HCUC model can successfully detect zero correlation and helps to mitigate the overestimation issue via the inclusion of the hysteresis effect. This result confirms the derivation above and our empirical study in section 3.2 that shows that the HCUC parameters are well identified, given enough moments from both recessions and expansions.

2.3 Bayesian estimation

The HCUC model in equations (1) through (6) is estimated using an MCMC method that approximates the posterior distributions of model parameters and unobserved components.[13] Let us denote $\boldsymbol{\phi} = (\phi_1, ..., \phi_p)'$, $\boldsymbol{\sigma} = (\sigma_\eta, \sigma_\epsilon, \rho)'$, $\boldsymbol{\delta} = (\tau_0, \mu_1, \mu_2, \boldsymbol{\beta}')'$, and $\boldsymbol{\theta} = (\boldsymbol{\phi}', \boldsymbol{\delta}', \boldsymbol{\sigma}')'$. We also define $\boldsymbol{y} = (y_1, ...y_T)'$, and $\boldsymbol{\tau}$, $\boldsymbol{c}$, $\boldsymbol{\eta}$, and $\boldsymbol{\epsilon}$ similarly. The MCMC sampler iterates over:

1. $\boldsymbol{\tau}, \boldsymbol{c} | \boldsymbol{y}, \boldsymbol{\theta}$,
2. $\boldsymbol{\theta} | \boldsymbol{y}, \boldsymbol{\tau}, \boldsymbol{c}$,

to generate draws from the posterior distribution $p(\boldsymbol{\tau}, \boldsymbol{c}, \boldsymbol{\theta} | \boldsymbol{y})$. In what follows we only discuss the first block since this highlights the novelty of the sampling for our model; while the sampling of the second block is more standard and is presented in the online appendix.

2.3.1 Sample $\boldsymbol{\tau}, \boldsymbol{c} | \boldsymbol{y}, \boldsymbol{\theta}$

The HCUC model can be written as:

$$\boldsymbol{y} = \boldsymbol{\tau} + \boldsymbol{c}, \tag{10}$$

$$\begin{bmatrix} \boldsymbol{H}_1 & \boldsymbol{H}_\beta \\ \boldsymbol{0} & \boldsymbol{H}_\phi \end{bmatrix} \begin{pmatrix} \boldsymbol{\tau} \\ \boldsymbol{c} \end{pmatrix} = \begin{pmatrix} \boldsymbol{\alpha} \\ \boldsymbol{0} \end{pmatrix} + \begin{pmatrix} \boldsymbol{\eta} \\ \boldsymbol{\epsilon} \end{pmatrix}, \quad \begin{pmatrix} \boldsymbol{\eta} \\ \boldsymbol{\epsilon} \end{pmatrix} \sim N\left(\boldsymbol{0}, \boldsymbol{\Sigma} \otimes \boldsymbol{I}_T\right), \tag{11}$$

where $\boldsymbol{I}_T$ is a $T \times T$ identity matrix. $\boldsymbol{H}_1$ and $\boldsymbol{H}_\phi$ are $T \times T$ lower-triangular sparse band matrices, both with ones on the main diagonal. $\boldsymbol{H}_1$ has minus ones on its lower diagonal; whereas $\boldsymbol{H}_\phi$

[13] We adopt a Bayesian estimation approach because in this way we can simultaneously take into account the estimation and filtering uncertainty. Likewise, we can also provide an intuitive and probabilistic interpretation of model comparison, which we discuss in section 3.4. However, in principle, it is also possible to use a Kalman filter-based frequentist approach to estimate the proposed HCUC model following, for example, Chapter 7 of Durbin and Koopman (2012).

has $-\phi_i$ on its i-th lower diagonal, $i = 1, ..., p$. Containing the hysteresis effect coefficients, $\boldsymbol{H}_\beta$ is a $T \times T$ lower-triangular sparse band matrix whose t-th row takes on the form

$$\left(\mathbf{0}_{1\times(t-k-1)}, -\beta_k \mathbb{1}_{\{t-k\in R\}}, ..., -\beta_1 \mathbb{1}_{\{t-1\in R\}}, \mathbf{0}_{1\times(T-t+1)}\right), \quad t = 1, ..., T.$$

In equation (11), $\boldsymbol{\alpha} = \left(\tau_0 + \mu_1, \mu_1 \mathbf{1}_{1\times(t_0-2)}, \mu_2 \mathbf{1}_{1\times(T-t_0+1)}\right)'$, where $\mathbf{1}$ is a matrix of ones with dimension indicated by its subscript, namely, $\boldsymbol{\alpha}$ specifies the initialization of potential output, and the pre- and the post-break potential output growth rates.

In the online appendix, we show that $(\boldsymbol{\tau}', \boldsymbol{c}')'$ in (11) is multivariate Gaussian and $\boldsymbol{c}|\boldsymbol{\theta}$ assumes a conditional Gaussian prior given by:

$$p(\boldsymbol{c}|\boldsymbol{\theta}) \propto \sigma_\epsilon^{-T} \exp\left(-\frac{1}{2\sigma_\epsilon^2} \boldsymbol{c}' \boldsymbol{H}_\phi' \boldsymbol{H}_\phi \boldsymbol{c}\right). \tag{12}$$

In the online appendix we also show that $\boldsymbol{\tau}$ assumes a conditional normal distribution, given $\boldsymbol{c}$ and $\boldsymbol{\theta}$. As a result, we can derive the conditional likelihood

$$p(\boldsymbol{y}|\boldsymbol{c}, \boldsymbol{\theta}) \propto \sigma_\eta^{-T} (1-\rho^2)^{-\frac{T}{2}} \exp\left(-\frac{1}{2(1-\rho^2)\sigma_\eta^2} (\boldsymbol{H}_1 \boldsymbol{y} - \boldsymbol{\alpha} - \boldsymbol{B}\boldsymbol{c})' (\boldsymbol{H}_1 \boldsymbol{y} - \boldsymbol{\alpha} - \boldsymbol{B}\boldsymbol{c})\right), \tag{13}$$

such that $\boldsymbol{y}|\boldsymbol{c}, \boldsymbol{\theta} \sim N\left(\boldsymbol{H}_1^{-1}\boldsymbol{\alpha} + \boldsymbol{H}_1^{-1}\boldsymbol{B}\boldsymbol{c}, (1-\rho^2)\sigma_\eta^2 (\boldsymbol{H}_1' \boldsymbol{H}_1)^{-1}\right)$ where $\boldsymbol{B} = \frac{\rho\sigma_\eta}{\sigma_\epsilon}(\boldsymbol{H}_\phi - \boldsymbol{H}_\beta) + \boldsymbol{H}_1$.

Combining (12) and (13), we can construct the conditional posterior distribution of the cycle:

$$\boldsymbol{c}|\boldsymbol{y}, \boldsymbol{\theta} \sim N\left(\frac{1}{(1-\rho^2)\sigma_\eta^2} \boldsymbol{K}_{\boldsymbol{c}}^{-1} \boldsymbol{B}' (\boldsymbol{H}_1 \boldsymbol{y} - \boldsymbol{\alpha}), \boldsymbol{K}_{\boldsymbol{c}}^{-1}\right), \tag{14}$$

where $\boldsymbol{K}_{\boldsymbol{c}} = \frac{1}{\sigma_\epsilon^2} \boldsymbol{H}_\phi' \boldsymbol{H}_\phi + \frac{1}{(1-\rho^2)\sigma_\eta^2} \boldsymbol{B}'\boldsymbol{B}$ is the precision matrix with a sparse and band structure. We use the precision sampler of Chan and Jeliazkov (2009) to efficiently draw $\boldsymbol{c}$ from the above conditional posterior, utilizing fast and low-memory inversion and Cholesky decomposition for sparse and band matrices. Subtracting the sampled cycle $\boldsymbol{c}$ from $\boldsymbol{y}$ gives a draw for the trend $\boldsymbol{\tau}$.

2.3.2 Prior distributions of static parameters

We assign independent priors for elements in $\boldsymbol{\phi}$, $\boldsymbol{\delta}$, and $\boldsymbol{\sigma}$. Specifically, $\boldsymbol{\phi} \sim N(\boldsymbol{\mu}^\phi, \boldsymbol{I}_p)\mathbb{1}_{\{\bar{\lambda}(\boldsymbol{\Phi})<1\}}$, with the prior mean $\boldsymbol{\mu}^\phi = (1.3, -0.7, \mathbf{0}_{1\times(p-2)})$ indicating an AR(2) cycle with complex roots (Hasenzagl et al., 2022). The condition $\mathbb{1}_{\{\bar{\lambda}(\boldsymbol{\Phi})<1\}}$ ensures stationarity: the largest eigenvalue of

$\boldsymbol{\Phi}$ in absolute value, denoted by $\bar{\lambda}(\boldsymbol{\Phi})$, is less than 1, where $\boldsymbol{\Phi}$ is the transition matrix of the AR(p) cycle put in the companion form.

Second, $\boldsymbol{\delta} \sim N(\boldsymbol{\mu}^{\delta}, \boldsymbol{V}^{\delta})$, where $\boldsymbol{\mu}^{\delta} = (750, 0.75, 0.375, \mathbf{0}_{1\times k})'$ and $\boldsymbol{V}^{\delta}$ is diagonal. The first three elements of $\boldsymbol{\mu}^{\delta}$ are the prior means of τ_0, μ_1 and μ_2 which are chosen based on Sinclair (2009), Grant and Chan (2017), and Eo and Morley (2022). These values imply that *a priori* hysteresis effects are absent and the annual growth rate of US real GDP is 3% before t_0 and 1.5% after. We follow the extensive model comparison results in Grant and Chan (2017) and fix the break date $t_0 =$ 2007:Q1. Large prior variances are used: $\boldsymbol{V}^{\delta}_{11} = 100$, $\boldsymbol{V}^{\delta}_{22} = \boldsymbol{V}^{\delta}_{33} = 1$, and $\boldsymbol{V}^{\delta}_{ii} = 10$ for $i \geq 4$. Regarding the COVID-19 distortion, we simply treat the observation $y_{2020:Q1}$ as missing so that the estimated COVID effect is $\text{COVID}|\boldsymbol{y} = y_{2020:Q1} - (\tau_{2020:Q1} + c_{2020:Q1})|\boldsymbol{y}$. This is equivalent to the dummy variable treatment $y_t = \tau_t + c_t + \nu \mathbb{1}_{\{t=2020:Q1\}}$, where the coefficient has a flat prior $\nu \sim N(0, \infty)$.

Lastly, we use $\sigma_\eta, \sigma_\epsilon \sim U[0, 3]$, and $\rho \sim U[-1, 1]$. Hence, $p(\boldsymbol{\sigma})$ is flat over the specified interval. We consider the uniform prior for variances more appealing than the inverse gamma prior because it does not exclude zero *a priori* and has a wider admissible range than what is commonly used in the literature. Sampling details are presented in the online appendix.

2.4 Model's extensions

2.4.1 The H^{l}CUC model: HCUC with real-time recession dates

In section 2.1, the choice of R is based on NBER-dated recessions. Because NBER recession dates are determined with a lag, the use of future data may introduce endogeneity issues into the model—specifically, reverse causality. Although we included two extra quarters before and after each recession to mitigate the timing issue, there is no guarantee that endogeneity completely disappears. A simple remedy is to use a real-time recession indicator. Hence, to address the reverse causality issue, we replace the NBER-dated recessions with the OECD-dated recessions. Based on a set of leading indicators of the US economy, OECD recession dates are determined by a turning point approach in real time (Gyomai and Wildi, 2013). We call this the H^{l}CUC model.

2.4.2 The H^{2}CUC model: HCUC with positive hysteresis

So far we have only considered the adverse recession effects associated with hysteresis effects. However, models that follow a Schumpeterian endogenous growth perspective have also emphasized the possible favorable effects associated with expansions.[14] To explore this possibility, we consider a HCUC model with two sets of $\boldsymbol{\beta}$ parameters: one for recessions and another for expansions. We call this extension the H^{2}CUC model. In this model, the time-varying drift in potential output is given by $\gamma_t = \mathbb{1}_{\{t<t_0\}}\mu_1 + \mathbb{1}_{\{t\geq t_0\}}\mu_2 + HE_t$, with

$$HE_t = \mathbb{1}_{\{t-1\in R\}}c_{t-1}\beta_1 + \mathbb{1}_{\{t-2\in R\}}c_{t-2}\beta_2 + \mathbb{1}_{\{t-1\notin R\}}c_{t-1}\beta_1^e + \mathbb{1}_{\{t-2\notin R\}}c_{t-2}\beta_2^e$$

defining the dynamic hysteresis effect such that $\boldsymbol{\beta}^e$ is an extra parameter vector that measures the effect of past cycles on potential output in non-recessionary periods. For identification, we set $p = 4$ and $k = 2$.

2.4.3 The H^{s}CUC model: HCUC with Markov switching

It is possible test for the presence or absence of hysteresis effects in an entirely model-consistent and data-driven specification. Hence, we consider a Markov regime switching HCUC model, which we call the H^{s}CUC model. This extension corresponds to a nonlinear HCUC model, where the determination of hysteresis effects is defined by a Markov process of two-state regime switches (Hamilton, 1989).

Let us denote $s_t = 1$ if the hysteresis effect is present at time t, and $s_t = 0$ if otherwise. The Markov regime switching is characterized by the following transition probabilities: $P(s_{t+1} = 0|s_t = 0) = q_{00}$, $P(s_{t+1} = 1|s_t = 0) = 1 - q_{00}$, $P(s_{t+1} = 1|s_t = 1) = q_{11}$, and $P(s_{t+1} = 0|s_t = 1) = 1 - q_{11}$. This results in the following dynamic hysteresis effect HE_t:

$$HE_t = s_{t-1}c_{t-1}\beta_1 + ... + s_{t-k}c_{t-k}\beta_k.$$

It is worth noting that this model differs from the Markov-switching state space models discussed by Kim (1994), which would imply $HE_t = s_t \sum_{i=1}^{k} c_{t-i}\beta_i$. A H^{s}CUC with $k = 4$ has

[14] For example, product varieties may increase as a result of higher investment during an expansion, which also stimulates R&D activities that positively affect potential output (Aghion et al., 2015). Some of the results reported by Mendieta-Muñoz (2017) support this view, who considered a different model specification.

$2^4 = 16$ states, rather than just 2 states. Due to the so-called "label-switching issue" caused by the large number of states (Kim, 1994), we do not use Hamilton filter-based methods for estimation (Hamilton, 1989). Instead, we develop a single-move sampler that computes the conditional posterior $p(\boldsymbol{s}|\boldsymbol{y}, \boldsymbol{c}, \boldsymbol{\delta}, \boldsymbol{\sigma}, \boldsymbol{q})$, where $\boldsymbol{s} = (s_1, ..., s_T)'$ and $\boldsymbol{q} = (q_{00}, q_{11})'$. For the transition probabilities, we assign conjugate Dirichlet priors as in Li and Mendieta-Muñoz (2022). Specifically, $(q_{00}, 1 - q_{00})' \sim Dir(e_1, e_2)$ and $(1 - q_{11}, q_{11})' \sim Dir(e_2, e_1)$ with $e_1 = 10$ and $e_2 = 1$. This implies that we assume persistent states with $q_{00} = q_{11} = 10/11$ *a priori*. The detailed sampling procedure is presented in the online appendix.

2.4.4 The H^{m}CUC model: HCUC with multivariate information

In section 2.2, we showed that all the parameters in the HCUC model can be identified given enough sample moments; however, we cannot recover either shock, even if theory-based restrictions (*e.g.*, long-run neutrality) are imposed. This is due to the fact that there are two shocks driving one observation, a common feature in UC models known as "excess shocks" discussed by Pagan and Robinson (2022) or "deformation" by Canova and Ferroni (2022).

Nevertheless, our main purpose is to focus on studying whether the available statistical evidence supports the presence or absence of hysteresis effects, instead of recovering demand or supply shocks. Assuming that $\boldsymbol{\beta}$ is positive and that during recessions the output gap is negative, the presence of the hysteresis effect can be corroborated if potential output is adversely affected by the output gap. Thus, our model specification extracts the parts of the cycle that permanently affect output—that is, HE_t as defined in (7); but it remains agnostic about the nature of the two shocks.

The results in Pagan and Robinson (2022) and Canova and Ferroni (2022) imply that it is impossible to recover supply and demand shocks in a univariate UC framework, so that any values of trend and cycle within the reported error bands are possible realizations of supply- and demand-driven fluctuations. As a result, the data used for model estimation greatly matters, as documented by the large literature that has pointed out that estimates of output gap are sensitive to the information set (see, for example, Basistha, 2007, Grant and Chan, 2017, Blanchard, 2018, González-Astudillo and Roberts, 2022 and Berger et al., 2023). As a robustness check and prior sensitivity analysis, we develop a multivariate extension of the baseline HCUC model, which

we call the H^{m}CUC model. In this model, the output gap c_t also affects the dynamics of other macroeconomic variables, so that c_t becomes a common factor driving several variables. In other words, we expand the information set in the estimation to measure more accurately the output gap. The H^{m}CUC model consists of equations (4) through (6) and

$$y_t^i = \tau_t^i + \kappa_1^i c_t + \kappa_2^i c_{t-1} + \psi_t^i,$$

where $i = (\pi_t, u_t, q_t)$, which indicates the year-on-year core CPI inflation, the unemployment rate, and the debt-service ratio (DSR), respectively. The use of π_t and u_t can be regarded as relevant for models' specifications that follow the Phillips curve and the Okun's law, respectively. Following Johnson and Li (2010), we include the DSR as a measure of the borrowing constraints and financial stress faced by US households, which we construct as the ratio of required household debt payments (sum of mortgage and consumer debt payments) to disposable income.

In this model, τ_t^i is an independent random walk for variable-specific trend, and $y_t^i - \tau_t^i$ is the gap component. These gaps have a factor structure with c_t as the common factor. The delayed common effect from c_{t-1} captures dynamic heterogeneous response among variables (Hasenzagl et al., 2022). Additionally, we specify the idiosyncratic components ψ_t^i's as correlated AR(2) processes, so that the cycles in the H^{m}CUC model have a generalized dynamic factor structure (Forni et al., 2000; Bai, 2003).[15]

Finally, as a prior sensitivity check for the proposed HCUC models, we assume that $\mathbf{\Sigma}$ and $\mathbf{\Sigma}^*$ in the H^{m}CUC model have inverse-Wishart priors centered at the identity matrix. The variances of η_t^i's are assigned independent gamma priors that do not exclude 0—so, *a priori*, variations in y_t^i's are assumed to come mainly from their cycles with independent idiosyncratic components. Sampling details are presented in the online appendix.

[15] In frequentist works, Forni et al. (2000) show that common factors can be identified despite the fact that a factor model has more shocks than observables; while Bai (2003) shows that the estimated common factors can be treated as being observed when the cross-sectional dimension is large. Future research may incorporate a larger set of variables, in which case Forni et al. (2000)'s finding ensures that c_t can be estimated even more precisely.

3 Estimating hysteresis effects in the US

Our empirical analysis for the US real GDP covers the period 1948:Q1-2022:Q3 for the baseline HCUC model, as well as for the variants UC, CUC, HUC, H^{2}CUC, H^{l}CUC, and H^{s}CUC models. Due to data availability, the period for the multivariate H^{m}CUC model begins in 1961:Q1. For all models we considered an AR(2) cycle, *i.e.*, $p = 2$ as in Morley et al. (2003), Sinclair (2009), Grant and Chan (2017), Li and Mendieta-Muñoz (2020), and Hasenzagl et al. (2022). We set $k = 4$. The estimation for each model is based on 70,000 MCMC iterations. The posterior sample is constructed from every fifth draw from the 50,000 MCMC draws with the first 20,000 burn-in periods discarded. We focus only on the presentation and discussion of the empirical results in this section; while we discuss the mixing property of the sampler in the online appendix, as well as the other relevant robustness checks. To summarize, the Markov chain shows satisfactory mixing with effective sample size larger than 10% of the posterior sample size.

The rest of this section comprises four parts. Section 3.1 presents the results regarding the estimated hysteresis effects, followed by sections 3.2, 3.3, and 3.4, which present the results associated with the potential output growth rate and the time-to-build effect, the output gap, and the Bayesian model comparison and averaging, respectively.

3.1 Dynamic hysteresis effects

Figure 1 presents the main results regarding the estimated dynamic hysteresis effect HE_t. The evolution of HE_t is strongly robust and consistent across models with different structures and prior settings. For example, by comparing the results obtained from the HCUC and the HUC models it is possible to observe that allowing for the innovations to be correlated does not affect the estimation of the dynamic hysteresis effect. Overall, significant downward movements in HE_t are observed during recessions.

Interestingly, the estimated cycle-generated movements lead to more important permanent drops in potential output only after the 1970s. Specifically, before 1970 a fall in HE_t during a recession was always followed by a rise of similar magnitude. This immediate recovery implies that potential output was not permanently affected. In other words, although c_t did affect τ_t via HE_t, potential output always went back to its pre-recession growing trajectory. Hence, the definition of hysteresis effects that emphasizes permanent losses in potential output is not

supported for this period. After the 1970s, however, the previously strong recovery pattern is no longer present: recession-induced losses in potential output growth become permanent since then. In figure 2 in section 3.1 of the online appendix, we also plot the cumulative hysteresis effect, showing that the drop in $\sum_{s=1}^{T} HE_s$ clearly occurs in the early 1970s. Indirectly, this finding offers evidence supporting the literature that considers 1973 as another structural break date for the US real GDP growth (see for example Grant and Chan, 2017).

The result above also confirms some of the findings of Furlanetto et al. (2021) and Benatti and Lubik (2022), who documented hysteresis for the US output mainly after, not before, the early 1980s, using different identification strategies. Following both studies, we also conducted three sub-sample exercises using 1970, 1980, and 1990 as the cut-off periods. The results presented in the online appendix show that there is only mild parameter instability when 1970 was selected as the cut-off point. Because HE_t is the sum of product terms $(\beta_i c_{t-i})$ as defined in equation (7), the different hysteresis effect coefficients in the early sample mean that the different behavior of HE_t pre- and post-1970s is unlikely caused by parameter instability, but rather by a change in the dynamics of the output gap. Thus, the sub-sample exercises further support our finding that the interaction between c_t and τ_t experienced a change in the early 1970s.

Additionally, it may be possible to argue that the absence of hysteresis effects before the 1970s was due to the more frequent and short-lived recessions. However, this view is not supported by the data. First, all models but H^{2}CUC have a constant $\boldsymbol{\beta}$. If earlier data points affecting $\boldsymbol{\beta}$ are in favor of a strong recovery, they should at least reduce the fall in HE_t post-1970s, which is at odds with the estimated evolution of HE_t. Second, the H^{m}CUC model considers a shorter period (from 1961:Q1 to 2022Q3), and still yields a fairly similar HE_t compared to the other HCUC models. Third, the real-time recessions (OECD recessions) used in the H^{l}CUC model have a higher frequency throughout the period—see the shaded area in the right panel of Figure 2, but this model still yields a fairly similar HE_t. Figure 2 further supports this finding by showing that the results obtained from the H^{s}CUC model do not depend on any pre-determined recessions: the estimated recession probability regime switches follow closely the NBER recessions (closer than the OECD recessions used in the H^{l}CUC model), only missing the recession of the early 1960s.

It is also important to point out that, when we allow for the possibility of positive hysteresis

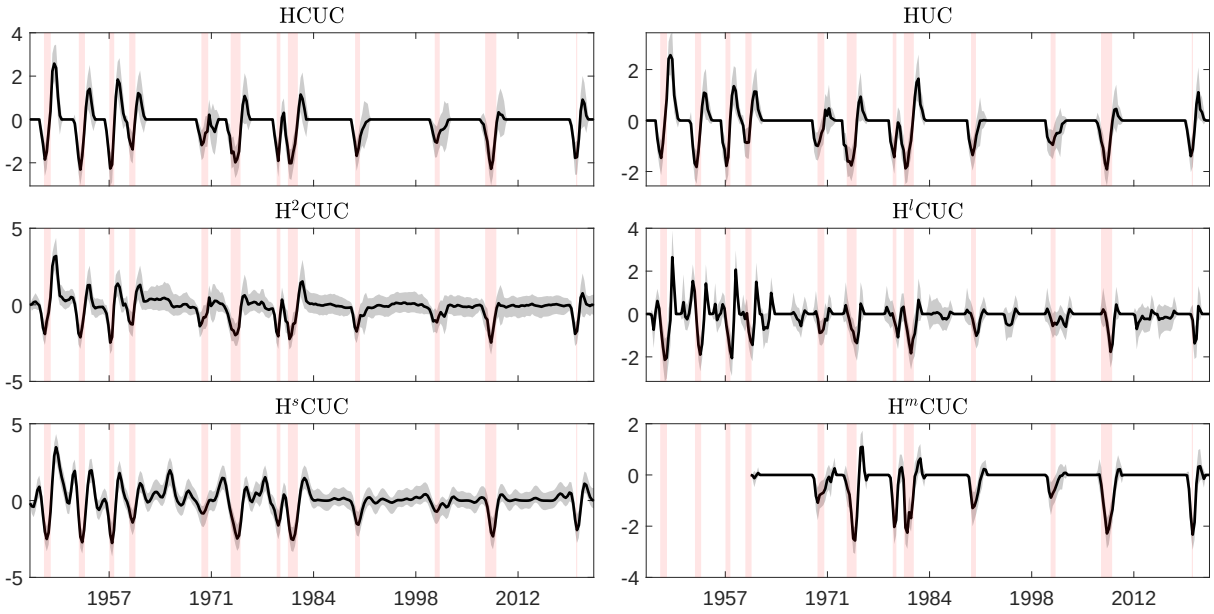

Figure 1: Dynamic hysteresis effect obtained from all models. We report the posterior median and 90% credible intervals of HE_t. The estimated HE_t shows the total effect of past cycles on potential output over time. Shaded areas indicate NBER recessions dates.

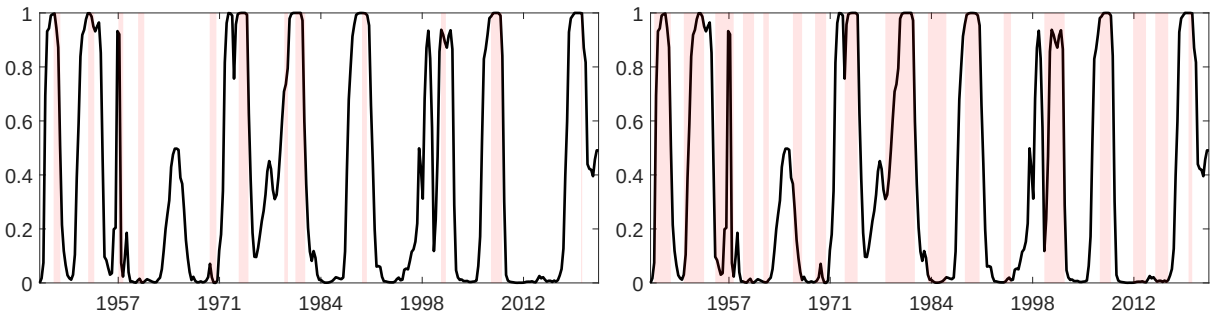

Figure 2: Estimated recession probability regimes obtained from the H^{s}CUC model. Posterior mean of recession probability regimes estimated from the H^{s}CUC model. Shaded areas indicate NBER recession dates (left) and OECD recession dates (right).

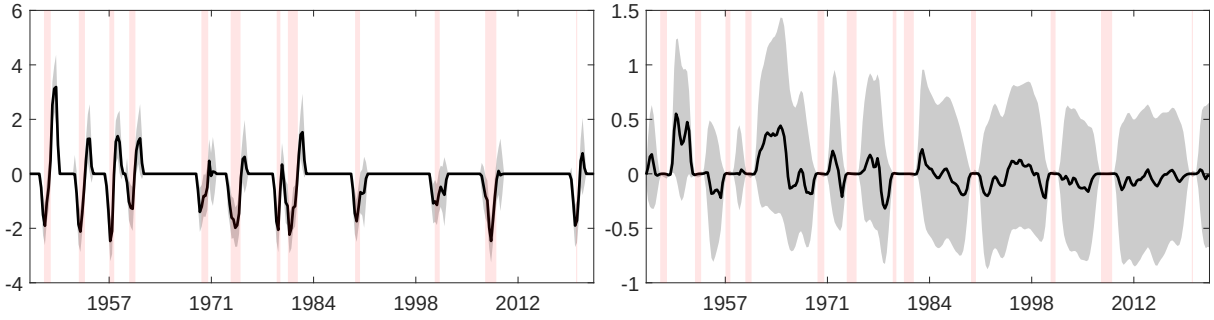

Figure 3: Dynamic hysteresis effect obtained from the H^{2}CUC model. The H^{2}CUC model allows for two different effects of the cycle on potential output: during recessions and expansions. Left: HE_t during recessions. Right: HE_t during expansions.

effects, the estimated HE_t obtained from the H^{2}CUC model is still fairly similar to the one obtained from the HCUC model. This is more clearly shown in Figure 3, which shows the hysteresis effects associated with both recessions and expansions. While the recession-induced HE_t follows closely the HE_t obtained from the HCUC model, the expansion-induced HE_t is essentially zero with the wide credible band covering zero. This highlights the lack of statistical evidence supporting positive hysteresis effects in the post-World War II period.[16]

Table 2 reports the estimates of $\boldsymbol{\beta}$ obtained from the different models. Given the similarity between the estimated dynamic hysteresis effects, it may be counterintuitive to observe that the parameters are different across the models. Nevertheless, this can be explained by noticing that the estimation of c_t, unlike the estimated HE_t, is less robust to the models' structures.[17] Importantly, all HCUC models but the HUC model show that $\sum_i^4 \beta_i > 0$. Since the output gap is expected to be negative during a recession, this result highlights the existence of relevant hysteresis effects according to the great majority of the estimated models.

To check for posterior significance, we conduct a joint Bayesian test for no hysteresis effects: $H_0 : \boldsymbol{\beta} = \mathbf{0}$ vs. $H_1 : \boldsymbol{\beta} \neq \mathbf{0}$. Following Kass and Raftery (1995), we compare the marginal data likelihood (MDL) under H_1 to the one under H_0 using the Bayes factor ($BF_{1,0}$):

$$BF_{1,0} = \frac{p(\boldsymbol{y}|H_1)}{p(\boldsymbol{y}|H_0)} = \frac{p(\boldsymbol{\beta} = \mathbf{0}|\boldsymbol{y})}{p(\boldsymbol{\beta} = \mathbf{0})}.$$

The right-hand side of the equation above is the Savage-Dickey density ratio that equals the ratio of the posterior ordinate at zero (the hypothesized value) to the prior ordinate at zero.[18] The posterior $p(\boldsymbol{\beta}|\boldsymbol{y})$ can be obtained from the MCMC samples; whereas the prior $p(\boldsymbol{\beta})$ is Gaussian, as specified in section 2.3.2. Thus, we compute the log Bayes factors for all models and compare them with the scale reported in Kass and Raftery (1995).

These results are reported at the bottom of table 2. From the latter it is possible to conclude that there is decisive evidence against $\boldsymbol{\beta} = \mathbf{0}$ for all models, which is consistent with the results plotted in figure 1 and with the fact that we found that $\sum_i^4 \beta_i > 0$.

[16] The only exception is the decade-long expansion in the 1960s, where the posterior mean of the expansion-induced HE_t does not include zero. This is partly consistent with the increase in the probability of an expansion regime estimated by the H^{s}CUC model, as shown in Figure 2. However, this probability is only approximately 0.5.

[17] We return to this discussion in section 3.3.

[18] The Savage-Dickey density ratio simplifies Bayesian testing for nested models, but it cannot be used for model comparison. In section 3.4 and in the online appendix, we derive formulas for computing the MDL of the proposed HCUC models.

Table 2: Hysteresis effect coefficients

	HCUC	HUC	H^{2}CUC	H^{l}CUC	H^{s}CUC	H^{m}CUC
β_1	**0.57** (0.22) [0.32, 0.88]	**−0.75** (0.30) [−1.15, −0.40]	**0.39** (0.20) [0.230, 0.77]	0.03 (0.13) [−0.14, 0.19]	**0.73** (0.19) [0.53, 0.94]	**0.28** (0.20) [0.13, 0.47]
β_2	**0.46** (0.23) [0.23, 0.81]	−0.13 (0.25) [−0.46, 0.17]	**0.34** (0.16) [0.09, 0.50]	**0.19** (0.16) [0.14, 0.39]	**0.36** (0.28) [0.13, 0.62]	**0.81** (0.30) [0.42, 1.17]
β_3	**0.71** (0.26) [0.39, 1.02]	**−0.27** (0.15) [−0.58, −0.13]	–	**−0.17** (0.14) [−0.28, −0.09]	−0.13 (0.23) [−0.44, 0.18]	0.22 (0.28) [−0.13, 0.59]
β_4	−0.02 (0.20) [−0.28, 0.25]	**−0.17** (0.18) [−0.30, −0.09]	–	**0.12** (0.12) [0.05, 0.23]	**−0.24** (0.13) [−0.37, −0.14]	**−0.49** (0.23) [−0.78, −0.22]
Bayesian joint test $H_0 : \boldsymbol{\beta} = \mathbf{0}$						
$\log BF_{1,0}$	11.23	12.08	9.82	7.15	9.64	18.57

Notes: We report the posterior medians, standard deviations in parentheses, and the 90% credible intervals in square brackets. Bold numbers indicate that the respective coefficient's credible interval does not include zero. The Bayesian joint test is based on the log Bayes factor computed by the Savage-Dickey density ratio. A value larger than 5 implies decisive evidence against the H_0.

3.2 Decline in potential output growth and the time-to-build effect

The first two columns of table 3 summarize the estimates of μ_1 and μ_2, or the potential output growth rates before and after the break in 2007:Q1 identified by Grant and Chan (2017).[19] We also include the results obtained from the standard UC and CUC models, besides the six models that allow for hysteresis effects. The HCUC model presents slightly higher median potential output growth rates compared to the CUC model: 3.8% (3.4%) before the 2007:Q1 break and 2.9% (1.7%) after. Thus, although the post-break growth rate rate is still lower than the pre-break rate, the decline is smaller. To illustrate this point further, the left panel of figure 4 shows the posterior distribution of the growth differential, $p(\mu_2 - \mu_1|\boldsymbol{y})$. It is possible to observe that the inclusion of the hysteresis effect reduces the difference. However, the 90% credible intervals of the differentials in all HCUC models still exclude zero, which means that hysteresis effect can potentially explain about 50% of the decline in potential output growth discussed in the literature on secular stagnation (see, for example, Gordon, 2015; Antolin-Diaz et al., 2017; Li and Mendieta-Muñoz, 2020). A similar result is shown in the last column of table 3, which

[19] Following the standard approach, we report the annualized growth rate.

computes the total decline in the potential output growth rate proxied by $\gamma_T - \gamma_1$. The decline in potential output growth is a robust finding across all model variants.

Table 3 shows two further important results. First, the different models yield similar estimates of τ_0. This is important because it shows that the unobserved components estimated from the HCUC models are not sensitive to the initialization parameters. Moreover, the COVID-19 effect is nearly identical across all model's variants, suggesting that our results are robust to this distortion (see the fifth column in table 3). Although we estimated the pandemic effect as a single outlier, its magnitude of -8.1% is very close to the -8.3% reported by Berger et al. (2023), who used a different modeling approach with a much larger information set.

Second, regarding the posterior estimate of the innovation correlation coefficient ρ that is attributed to the time-to-build effect, we find that, similar to Morley et al. (2003) and Grant and Chan (2017), the CUC model exhibits a high correlation coefficient, pointing to a single-source error dynamics.[20] However, when hysteresis effects are included, the correlation is reduced to -0.67 according to the HCUC model and to -0.5 according to the H^{m}CUC model, for example. Indeed, the right panel of figure 4 shows that all HCUC models present a lower ρ compared to the CUC model. Since the time-to-build effect refers to the contemporaneous output gap response to a positive technology (supply) shock, a model without hysteresis effects can erroneously identify every recession with a positive change in potential output, and every expansion with a negative change in potential output, which affects the estimates of the output gap. We observe that models that allow for both hysteresis effects and innovation correlation yield a lower correlation coefficient due to the different timing assumed for each of the effects. The following section shows that, by doing this, the counterintuitive output gap estimates derived from the CUC model can be improved.

3.3 Output gap

Since output gap estimation is one of the main reasons why unobserved components models have gained considerable popularity, we believe that it is important to discuss the results obtained

[20] It is possible to interpret this result as evidence that the time-to-build effect is the sole driver of business cycle fluctuations, so there is no demand-driven transitory movements in output. Morley et al. (2003) provide similar arguments from a statistical point of view. However, one can also think of this as a "correlation puzzle" because most new-Keynesian models have difficulties rationalizing the nearly perfect negative correlation. In this sense, it is difficult to believe either conceptually or empirically that all recessions are always associated with positive technology shocks.

Table 3: Annualized potential output growth rate, the time-to-build effect, and the COVID-19 effect

	$4 \times \mu_1$	$4 \times \mu_2$	ρ	COVID	τ_0	$4 \times (\gamma_T - \gamma_1)$
UC	3.38 (0.15) [3.21, 3.57]	1.62 (0.38) [1.14, 2.08]	–	−8.08 (0.51) [−8.71, −7.42]	761.3 (0.81) [760.2, 762.3]	−1.78 (0.42) [−2.31, −1.26]
CUC	3.36 (0.35) [2.93, 3.83]	1.66 (0.66) [0.83, 2.52]	−0.88 (0.04) [−0.92, −0.83]	−8.14 (0.51) [−8.78, −7.44]	761.1 (0.70) [760.3, 762.0]	−1.69 (0.79) [−2.62, −0.71]
HCUC	3.79 (0.31) [3.39, 4.19]	2.94 (0.43) [2.34, 3.50]	−0.67 (0.06) [−0.74, −0.59]	−8.05 (0.56) [−8.72, −7.34]	760.7 (0.72) [759.8, 761.6]	−1.74 (0.75) [−2.52, −0.94]
HUC	3.67 (0.25) [3.39, 3.95]	2.60 (0.37) [2.11, 3.08]	–	−8.01 (0.54) [−8.70, −7.32]	760.8 (0.79) [759.8, 761.8]	−1.68 (0.66) [−2.21, −1.05]
H^2CUC	3.79 (0.45) [3.36, 4.08]	2.93 (0.73) [2.52, 3.57]	−0.72 (0.07) [−0.80, −0.62]	−8.09 (0.58) [−8.81, −7.30]	760.9 (0.64) [760.0, 761.6]	−1.72 (0.87) [−2.24, −1.01]
H^lCUC	3.48 (0.61) [3.30, 3.89]	2.23 (0.55) [1.84, 2.80]	−0.62 (0.07) [−0.71, −0.52]	−8.19 (0.72) [−9.09, −7.28]	760.9 (0.83) [759.1, 762.6]	−1.75 (0.81) [−2.28, −1.13]
H^sCUC	3.58 (0.96) [3.31, 3.82]	2.17 (1.02) [1.41, 2.84]	−0.74 (0.10) [−0.85, −0.59]	−8.08 (0.55) [−8.79, −7.40]	760.7 (0.90) [759.6, 761.8]	−1.83 (1.17) [−2.71, −1.26]
H^mCUC	3.59 (0.49) [2.98, 4.18]	2.61 (0.66) [1.82, 3.53]	−0.53 (0.07) [−0.59, −0.44]	−8.17 (0.49) [−8.83, −7,57]	807.5 (0.71) [806.6, 808.4]	−1.32 (0.97) [−2.16, −0.51]

Notes: We report the posterior medians, standard deviations in parentheses, and the 90% credible intervals in square brackets. The estimation period for the H^mCUC model is 1961:Q1-2022:Q3. For the rest of the models, the estimation period is 1941:Q1-2022:Q3.

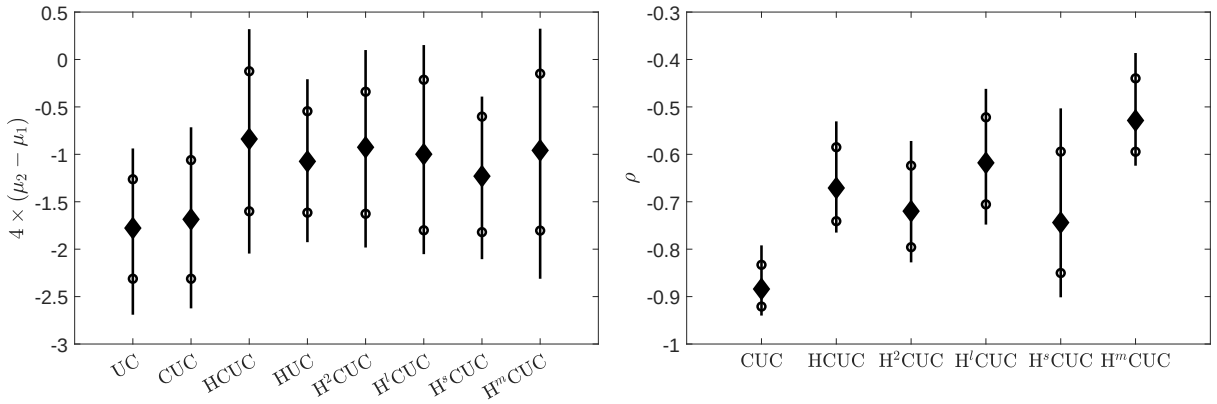

Figure 4: Differences in annualized potential output growth rates and the time-to-build effect before and after 2007:Q1. Left: The posterior median distributions of the potential growth rates, $\mu_2 - \mu_1$, obtained from the different models. Right: The posterior median distributions of the innovation correlation coefficients, ρ, for the different models. All results are summarized by the range (vertical bar), the 90% posterior interval (circles), and the median (diamond).

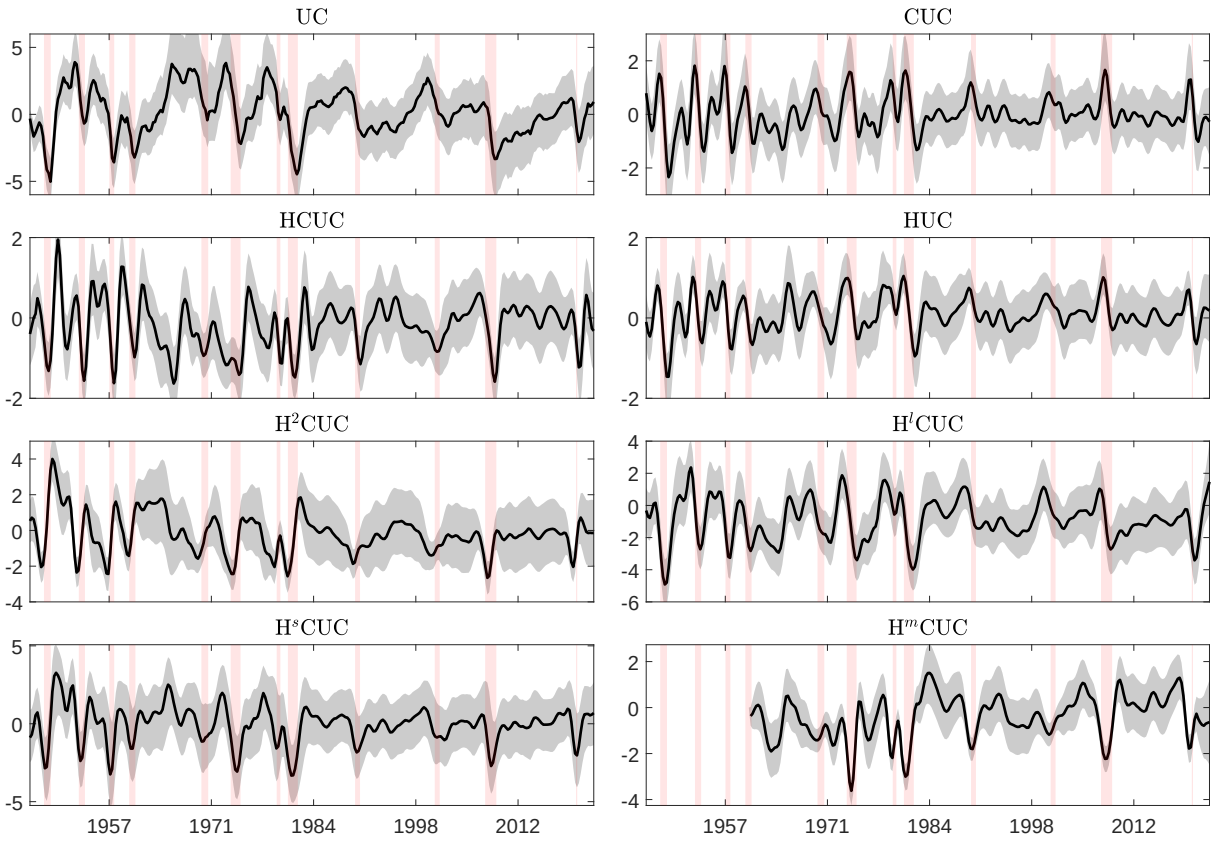

Figure 5: Output gap estimates. We report the posterior medians and the 90% credible intervals of the estimated output gap c_t for each model. The output gap corresponds to the log difference between observed and potential output. Shaded areas indicate NBER recessions dates.

from the proposed HCUC models. The posterior distribution of the cycle c_t is shown in figure 5. The eight estimates can be classified into three main groups: UC, CUC, and HCUC models.

The UC output gap is similar to the one obtained from the Hodrick-Prescott filter, which has been extensively discussed (Harvey and Shephard, 1993; Durbin and Koopman, 2012). On the other hand, the CUC model (popularized by the works of Morley et al., 2003, Sinclair, 2009, and Grant and Chan, 2017, among others) is closely related to the Beveridge-Nelson decomposition (Beveridge and Nelson, 1981), and it seems to yield a counterintuitive estimate of the economists' understanding of cyclical fluctuations. Consider the 2007-9 Global Financial Crisis (GFC), for example. At the beginning of the recession, c_t experiences an important increase, and during the course of the recession it falls to zero.

There are two possible explanations for this result. First, the high correlation coefficient between innovations or time-to-build effect. Second, the excess trend volatility σ_η reported in table 4. These effects imply that, when a recession takes place, the fall in output is largely

attributed to the trend component due to $\sigma_\eta > \sigma_\epsilon$. To compensate for the sudden fall in τ_t, the large negative correlation coefficient ρ causes an increase (rather than a decrease) in c_t as a result. As mentioned above, this "negative time-to-build effect" is hard to justify theoretically, and it also contradicts some of the literature that shows that the GFC generated a large negative demand shock, at least at the beginning of the recession—see, *e.g.*, Bashar (2011), Adrian et al. (2019), and Eo and Morley (2022). Similarly, the CUC output gap increases at the beginning of the COVID-19 recession, which is, again, due to the combined effect of a negative time-to-build effect and a higher trend volatility.

We point out that the HUC output gap is close to the one obtained from the CUC model. Using equation (8), it can be shown that, if the cycle follows an AR(2) process, an HUC model with $c_t\beta$ and another one with $c_{t-1}\beta$ affecting the dynamics of γ_t in (5) yield an identical reduced-form ARIMA(2,1,2) representation of the CUC model. For these three models, equation (9) matches three structural parameters, either $(\sigma_\eta^2, \sigma_\epsilon^2, \beta)$ or $(\sigma_\eta^2, \sigma_\epsilon^2, \rho\sigma_\eta\sigma_\epsilon)$, with the first three autocovariances in the reduced-form MA errors. This suggests that, even if the HUC model includes an extra lag in HE_t, its CUC-equivalent reduced-form estimates only the time-to-build effect. Hence, including either the hysteresis effect or the time-to-build effect in the estimation is insufficient to generate models that satisfactorily capture output dynamics.[21]

Therefore, by introducing simultaneously the hysteresis effect and the correlation between innovations via different timings, the HCUC models effectively alleviate this tension and yield more consistent and intuitive output gap estimates. This can be summarized by three results. Firstly, the estimated output gaps are robust across the different HCUC models.

Secondly, the implied cycle periodicity (or the inverse of the implied cycle frequency), reported in table 4 (column four) shows that the UC model yields approximately 6.9 years between recessions, largely in line with the economists' understanding of the business cycle frequency; whereas the CUC and the HUC model yield a periodicity of less than two years.[22] This is, again, due to the large negative correlation coefficient and excess trend volatility that make the cycle persistence very low. If the standard CUC model is augmented with hysteresis effects as in the HCUC model, the estimated persistence leads to a two-year increase in cycle periodicity.

[21] This also explains why $\sum_i^4 \beta_i$ in the HUC model is negative, as shown in table 2.

[22] For a stationary AR(2) process with complex roots, the implied periodicity can be computed from its spectral density (see also Harvey and Shephard, 1993 and Hasenzagl et al., 2022). For quarterly data, the implied cycle periodicity in number of years is $0.5\pi/\arccos(\phi_1/\sqrt{-4\phi_2})$.

Table 4: Autoregression coefficients and standard deviation of the innovations

	ϕ_1	ϕ_2	Period*	σ_η	σ_ϵ	$p(\sigma_\eta > \sigma_\epsilon \mid \boldsymbol{y})$
UC	1.49 (0.09) [1.38, 1.60]	−0.56 (0.10) [−0.68, −0.43]	6.90 (3.13) [4.81, 14.67]	0.55 (0.09) [0.41, 0.64]	0.60 (0.09) [0.50, 0.74]	0.381
CUC	0.68 (0.15) [0.51, 0.91]	−0.30 (0.11) [−0.44, −0.15]	1.81 (0.92) [1.51, 2.38]	1.37 (0.11) [1.22, 1.51]	0.90 (0.16) [0.74, 1.13]	0.942
HCUC	0.83 (0.10) [0.70, 0.97]	−0.19 (0.09) [−0.33, −0.08]	3.76 (1.86) [2.91, 6.28]	0.95 (0.11) [0.83, 1.12]	0.88 (0.12) [0.72, 1.08]	0.655
HUC	1.09 (0.14) [0.91, 1.27]	−0.58 (0.13) [−0.74, −0.41]	1.93 (1.29) [1.37, 3.73]	0.50 (0.06) [0.43, 0.57]	0.41 (0.08) [0.32, 0.51]	0.813
H^2CUC	1.03 (0.18) [0.81, 1.33]	−0.32 (0.08) [−0.40, −0.22]	3.62 (2.18) [2.15, 6.60]	0.93 (0.10) [0.75, 1.03]	0.81 (0.15) [0.61, 1.01]	0.688
H^lCUC	1.17 (0.16) [0.97, 1.40]	−0.36 (0.12) [−0.53, −0.27]	4.15 (1.66) [3.08, 7.21]	0.85 (0.08) [0.68, 1.20]	0.53 (0.12) [0.39, 0.72]	0.723
H^sCUC	1.21 (0.12) [1.08, 1.50]	−0.48 (0.16) [−0.61, −0.28]	3.28 (2.46) [1.87, 5.22]	1.05 (0.13) [0.91, 1.30]	0.89 (0.17) [0.63, 1.11]	0.704
H^mCUC	1.41 (0.10) [1.29, 1.64]	−0.47 (0.08) [−0.56, −0.36]	4.87 (2.75) [3.18, 9.46]	0.61 (0.07) [0.52, 0.74]	0.83 (0.15) [0.65, 1.10]	0.240

Notes: We report the posterior medians, the standard deviations in parentheses, and the 90% credible intervals in square brackets.

* Refers to the implied cycle periodicity computed from the complex AR polynomial roots. The few MCMC iterations associated with real roots of the AR polynomial were discarded. The values reported refer to number of years.

Thirdly, the HCUC models mitigate the excess trend volatility by allocating part of the trend volatility to past cyclical fluctuations via dynamic hysteresis effects. For the same level of variation in potential output growth, the models reduce σ_η, so that the posterior probability of excess trend volatility is also reduced, as shown by the last column of table (4).

Lastly, we highlight two features regarding the H^mCUC model. First, the output gap generated by this model can be considered as a measure of the business cycle corresponding to the common factor among nominal, real, and financial variables. As shown in figure 5, the credible error band of c_t obtained from this model is narrower, suggesting that the output gap is estimated more accurately when we use an extended information set, as predicted by Forni et al. (2000) and Bai (2003). Second, table (4) shows that the posterior probability of excess trend volatility in this model is even lower than in the UC model, which suggests that most of

the variation in output comes from the cycle and not from its long-run potential level.

3.4 Model comparison and averaging

From a Bayesian estimation approach, the MDL provides a direct way to assess model uncertainty by showing how likely the observed data is generated by a specific model. For a given model M with trend $\boldsymbol{\tau}$, cycle $\boldsymbol{c}$, and static parameter vector $\boldsymbol{\theta}$, the MDL is given by

$$p(\boldsymbol{y}|M) = \int p(\boldsymbol{y}|\boldsymbol{\theta}, M)p(\boldsymbol{\theta}|M)d\boldsymbol{\theta} \approx \frac{1}{N}\sum_{i}^{N} p(\boldsymbol{y}|\boldsymbol{\theta}^{(i)}, M), \tag{15}$$

where $p(\boldsymbol{\theta}|M)$ is the prior distribution; and $p(\boldsymbol{y}|\boldsymbol{\theta}, M) = \int p(\boldsymbol{y}|\boldsymbol{c}, \boldsymbol{\theta})p(\boldsymbol{c}|\boldsymbol{\theta})d\boldsymbol{c}$ is the integrated likelihood. The last term in equation (15) is the Monte Carlo integration, which is an unbiased estimator of $p(\boldsymbol{\theta}|M)$ where $\boldsymbol{\theta}^{(i)}$, $i = 1, ..., N$, is a draw from its prior.

In the online appendix, we show that the integrated likelihood for the HCUC, the H^{2}CUC, and the H^{l}CUC models can be derived following Grant and Chan (2017). The integrated likelihood includes functions of the sparse band matrices $\boldsymbol{B}$ and $\boldsymbol{K}_c$ from (13) and (14). We use the efficient band matrix routine in Chan and Jeliazkov (2009) to calculate the integrated likelihood, which is the main element for computing the MDL in equation (15).[23]

To compute the MDL of the nonlinear H^{s}CUC model, we consider a sequential Monte Carlo procedure, the details of which are also presented in the online appendix. For the multivariate H^{m}CUC model, we consider the conditional data likelihood $p(\boldsymbol{y}|\boldsymbol{y}_2)$, with $\boldsymbol{y}_2$ collecting variables other than the log real GDP. The associated conditional integrated likelihood is $\int p(\boldsymbol{y}|\boldsymbol{y}_2, \boldsymbol{c})d\boldsymbol{c}$, and it can be readily computed given the linear and Gaussian model structure.

Table 5 summarizes the results by reporting the log Bayes factor of model M relative to the UC model, which corresponds to $\log BF_{\mathrm{M,UC}} = \log p(\boldsymbol{y}|M) - \log p(\boldsymbol{y}|\mathrm{UC})$.[24] Considering the period 1961:Q1-2022Q3 and $N = 10,000$, we find that $\log p(\boldsymbol{y}|\mathrm{UC}) = -344.76$. The table shows that there is decisive evidence in favor of both the hysteresis effect and correlated innovations, with the former generating a more important marginal likelihood improvement. Also, with the exception of the H^{m}CUC model, additional model structure does not seem to improve considerably the model fit of the US real GDP, as seen by the smaller log Bayes factor obtained

[23] The routine developed by Chan and Jeliazkov (2009) is considerably faster than the Kalman filter.

[24] It is also possible to interpret these results as the log MDL distance to the UC model. This means that model M is $\exp(\log BF_{\mathrm{M,UC}})$ times more likely than the UC model given the data.

Table 5: Model comparison

UC	CUC	HCUC	HUC	H^{2}CUC	H^{l}CUC	H^{s}CUC	H^{m}CUC
Log Bayes factor relative to the UC model: $\log BF_{\mathrm{M,UC}}$							
0	5.86	16.07	11.42	14.48	13.50	15.83	16.31
Posterior model probability: $P(M\|\boldsymbol{y})$							
0	0	0.30	0	0.06	0.02	0.24	0.38

Notes: We report the log Bayes factor of a specific model M relative to the UC model. The posterior model probability is computed by assuming that every model is equally likely *a priori*. A value larger than 5 implies decisive evidence in favor of model M.

from the HUC, H^{2}CUC, H^{l}CUC, and H^{s}CUC models relative to the HCUC model. This finding is consistent with the similar dynamic hysteresis effect and output gap estimates obtained from all these models, as presented in figures 1 and 5.

Since the incorporation of both hysteresis effects and the time-to-build effect via different timings is empirically important, we proceed to compute the posterior distribution using Bayesian model averaging (BMA) (Kass and Raftery, 1995), *i.e.*, the average of posterior distributions from different models weighted by their posterior model probabilities:

$$p(M|\boldsymbol{y}) \propto p(\boldsymbol{y}|M)p(M).$$

Assuming that all models are equally likely *a priori*, the posterior is simply proportional to the MDL. Therefore, we can compute the posterior model probabilities using the log Bayes factors. We report these at the bottom of table 5. Interestingly, the results show that: (i) the US real GDP is best described by the H^{m}CUC, HCUC, and the H^{s}CUC models; and (ii) the CUC and HUC models receive smaller weights compared to the models where $\rho \neq 0$ and $\boldsymbol{\beta} \neq 0$.

Finally, using the Bayes rule, the BMA posterior distribution of $\boldsymbol{x}$ can be constructed as:

$$p^{\mathrm{BMA}}(\boldsymbol{x}|\boldsymbol{y}) = \sum_{i=1}^{m} p(M_i|\boldsymbol{y})p(\boldsymbol{x}|\boldsymbol{y}, M_i), \tag{16}$$

where $\boldsymbol{x}$ is either the output gap or the dynamic hysteresis effect, m is the total number of models, and draws from $p^{\mathrm{BMA}}(\boldsymbol{x}|\boldsymbol{y})$ consist of draws from $p(\boldsymbol{x}|\boldsymbol{y}, M_i)$ with probability $p(M_i|\boldsymbol{y})$.

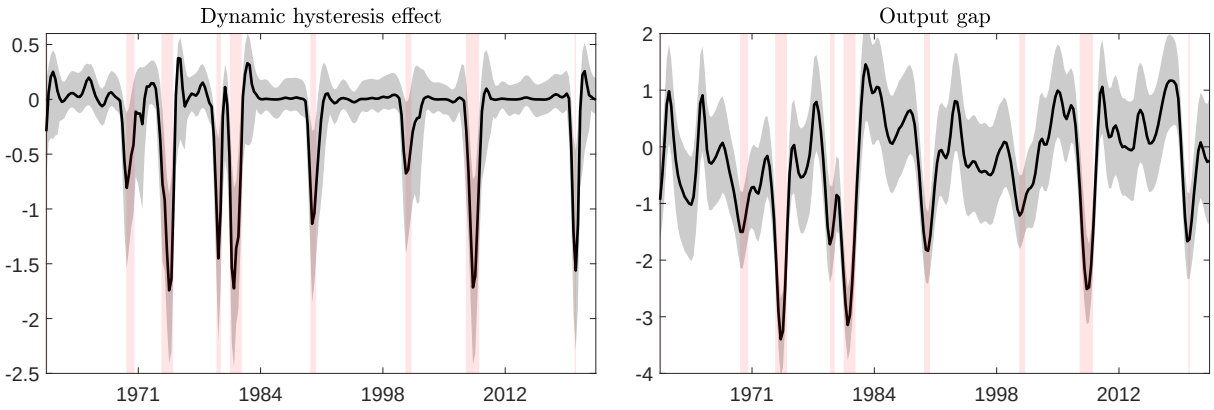

Figure 6: Average dynamic hysteresis effect and output pap for all HCUC models. Reported are the Bayesian model averaging (BMA) posterior medians and the 90% credible intervals of the estimated dynamic hysteresis effect and the output gap obtained from the HCUC models. Shaded areas indicate NBER recessions dates.

Figure 6 shows the dynamic hysteresis effect and output gap obtained from the BMA for the HCUC models according to equation (16), considering the period 1961:Q1-2022:Q3. The evolution of both components largely confirms the previous findings obtained from the baseline HCUC model. Notice that the credible intervals of both the hysteresis effect and the output gap estimates are now narrower than the ones for the HCUC model shown in figures 1 and 5, respectively, so that the uncertainty associated with the estimation of the hysteresis effect and output gap can be further reduced via BMA.

4 Policy implications

Perhaps the most important finding presented in the previous section is that hysteresis effects have become more relevant for the US economy since the early 1970s, so that recessions have progressively affected the evolution of potential output growth since then.[25] This result provides further relevance to the growing research that has begun to explore the implications of hysteresis effects for welfare analysis (Tervala, 2021) and for the optimal implementation of fiscal policy (Engler and Tervala, 2018; Tervala and Watson, 2022) and monetary policy (Garga and Singh, 2021; Acharya et al., 2022; Fatás and Singh, 2022; Galí, 2022).

[25] A comprehensive discussion and modeling of the social and economic reasons that ultimately explain this result is beyond the scope of our article. However, the channels emphasized by Benigno and Fornaro (2018)—namely, weak aggregate demand that affect agents' expectations of future growth—and Herrendorf et al. (2014) and Duernecker et al. (2021)—*i.e.*, the structural transformation of the US economy and the reallocation of economic activity across the broad sectors agriculture, manufacturing, and services—can help to identify the underlying causes of the changing relevance of hysteresis effects in future research.

To summarize, since our findings support the presence of hysteresis effects, aggressive and timely stabilization policies—both fiscal and monetary, conventional and unconventional—should be prioritized during recessions. This conclusion resonates with Yellen (2016) and has three immediate implications for the future behavior of policy makers. First, overall, inflation stabilization during recessions must be considered of secondary importance. This is extremely relevant because, as shown by Tervala (2021), the welfare costs of recessions are considerably larger if hysteresis effects are explicitly modeled.[26]

Second, both fiscal and monetary policies can play an important role to decrease the deleterious effects associated with hysteresis effects. With respect to the former, Engler and Tervala (2018) and Tervala and Watson (2022) show that in the presence of hysteresis: (i) the fiscal output multiplier is much larger and the welfare multiplier of fiscal policy—that is, the consumption equivalent change in welfare for one dollar change in public spending—is positive; and (ii) public investment possesses larger output and welfare multipliers than government transfers and public consumption. This implies that temporary fiscal stimulus—mainly associated with public investment—have high output and welfare multipliers that help limit the long-run damages of recessions on potential output by strengthening the recoveries.[27]

Regarding the relevance of monetary policy, it is possible to highlight the following for an hysteresis-prone economy: (i) given the zero lower bound, the study of unconventional policies that can alleviate the relevant commitment concerns faced by the central bank is a promising agenda for future research (Garga and Singh, 2021); (ii) the timing of monetary policy matters significantly for long-run outcomes because timely commitment to future accommodative policy early in a recession can prevent hysteresis from happening and enable a swift recovery (Acharya et al., 2022); (iii) since potential output becomes harder to define, the central bank faces significant challenges if monetary policy is not aggressive enough in response to adverse demand shocks (Fatás and Singh, 2022); and (iv) optimal monetary policy requires a more aggressive stabilization of output (unemployment) than the one implied by a conventional interest rate rule, and monetary policy strategies that put too much weight on inflation stabilization can be inefficient (Galí, 2022). Thus, the presence of hysteresis has two main

[26] Specifically, Tervala (2021) focuses on total factor productivity hysteresis—*i.e.*, demand-driven changes in employment that can permanently affect total factor productivity in a New Keynesian model.

[27] Alternatively, this implies that, during weak economic conditions, the detrimental effects of fiscal consolidation are considerable because of the presence of hysteresis effects.

implications for the current implementation of monetary policy: (i) central bankers should respond aggressive enough to adverse demand shocks, perhaps via unconventional monetary policies; and (ii) delayed monetary policy interventions may be powerless to bring the economy back to full employment since these generate policy errors that can be larger and more difficult to amend in the future.

Third, the stabilization policies discussed above can also have an important role to play to counteract the decline in potential output growth found by the literature on secular stagnation—see, for example, Gordon (2015), Fernald et al. (2017), Antolin-Diaz et al. (2017) and Li and Mendieta-Muñoz (2020), among others. In other words, both fiscal and monetary policies are likely to be beneficial for long-run economic growth rates in the US if implemented appropriately during future recessions.

5 Conclusions

This article presents novel models and methods aimed at estimating the long-run effects associated with recessions over time, *i.e.*, dynamic hysteresis effects. By incorporating different timings in the structure of unobserved components models, we show that it is possible to disentangle the long-run adverse effects associated with recessions from other relevant effects that may also exist when studying the interactions between cycles and trends in output—such as time-to-build effects in the context of CUC models. The proposed baseline model is called the HCUC model, which explicitly captures two relevant features of an economy: it incorporates non-neutrality in the long-run by introducing dynamic hysteresis effects and it considers time-to-build effects by modeling the correlation between permanent and transitory innovations. We also provide extensions of the HCUC model by developing models that: (i) separate the effects of recessions and expansions; (ii) consider a real-time recession indicator; (iii) introduce nonlinear effects via Markov regime switching; (iv) consider a multivariate framework; and (v) contain alternative priors.

Using Bayesian estimation methods, we find two main results that are robust across all estimated models for the US economy. First, recessions have reduced potential output growth since the early 1970s, so that hysteresis effects have become more relevant to understand the dynamics of output since then. Second, compared to CUC models, the HCUC models: (i)

estimate a lower correlation coefficient between permanent and transitory innovations—that is, a smaller time-to-build effect; (ii) yield more consistent and intuitive output gap estimates; and (iii) improve the model fit of the US real GDP according to Bayesian model comparison methods. These results emphasize the increasing importance of studying cyclical long-run non-neutral effects and stress that our understanding of the interactions between cycles and trends can be improved by considering the hysteresis and time-to-build effects as two different economic phenomena.

References

Acharya, S., Bengui, J., Dogra, K., and Wee, S. L. (2022) "Slow recoveries and unemployment traps: Monetary policy in a time of hysteresis." *Economic Journal* **132**, 2007-2047.

Adrian, T., Boyarchenko, N., and Giannone, D. (2019) "Vulnerable growth." *American Economic Review* **109**, 1263-1289.

Aghion, P., Akcigit, U., and Howitt, P. (2015) "Lessons from Schumpeterian growth theory." *American Economic Review* **105**, 94-95.

Antolin-Diaz, J., Drechsel, T. and Petrella, I. (2017) "Tracking the slowdown in long-run GDP growth." *Review of Economics and Statistics* **99**, 343-356.

Bai, J. (2003) "Inferential theory for factor models of large dimensions." *Econometrica* **71**, 135-171.

Bakas, D., and Mendieta-Muñoz, I. (2020) "Financial crises and economic recovery: Cross-country heterogeneity and cross-sectional dependence." *Economics Letters* **195**, 109435.

Ball, L. (2009) "Hysteresis in unemployment: Old and new evidence." *National Bureau of Economic Research (NBER) Working Paper* **14818**.

Ball, L. (2014) "Long-term damage from the Great Recession in OECD countries." *European Journal of Economics and Economic Policies: Intervention* **11**, 149-160.

Bashar, O. (2011) "On the permanent effects of an aggregate demand shock: Evidence from the G-7 countries." *Economic Modelling* **28**, 1374-1382.

Basistha, A. (2007) "Trend-cycle correlation, drift break and the estimation of trend and cycle in Canadian GDP." *Canadian Journal of Economics* **40**, 584-606.

Benatti, L., and Lubik, T. A. (2022) "Searching for hysteresis." *Federal Reserve Bank of Richmond Working Paper* **22-05**.

Benigno, G., and Fornaro, L. (2018) "Stagnation traps." *Review of Economic Studies* **85**, 1425-1470.

Berger, T., Morley, J., and Wong, B. (2023) "Nowcasting the output gap." *Journal of Econometrics* **232**, 18-34.

Beveridge, S., and Nelson, C. R. (1981) "A new approach to decomposition of economic time series into permanent and transitory components with particular attention to measurement of the 'business cycle'." *Journal of Monetary Economics* **7**, 151-174.

Blanchard, O. and Quah, D. (1989) "The dynamic effects of aggregate demand and supply disturbances." *American Economic Review* **79**, 655-673.

Blanchard, O., Cerutti, E., and Summers, L. (2015) "Inflation and activity—Two explorations and their monetary policy implications." *International Monetary Fund (IMF) Working Paper* **WP/15/230**.

Blanchard, O. (2018) "Should we reject the natural rate hypothesis?" *Journal of Economic Perspectives* **32**, 97-120.

Canova, F., and Ferroni, F. (2022) "Mind the gap! Stylized dynamic facts and structural models." *American Economic Journal: Macroeconomics* **4**, 104-135.

Cerra, V., and Saxena, S. C. (2008) "Growth dynamics: The myth of economic recovery." *American Economic Review* **98**, 439-457.

Cerra, V., Fatás, A., and Saxena, S. C. (2023) "Hysteresis and the business cycle." *Journal of Economic Literature* **61**, 181-225.

Chan, J. C., and Jeliazkov, I. (2009) "Efficient simulation and integrated likelihood estimation in state space models." *International Journal of Mathematical Modelling and Numerical Optimisation* **1**, 101-120.

Cover, J., Enders, W. and Hueng, J. (2006) "Using the aggregate demand-aggregate supply model to identify structural demand-side and supply-side shocks: Results using a bivariate VAR." *Journal of Money, Credit and Banking* **38**, 777-790.

Duernecker, G., Herrendorf, B. and Valentinyi, Á. (2021) "The productivity growth slowdown and Kaldor's growth facts." *Journal of Economic Dynamics and Control* **130**, 104200.

Dungey, M., Jacobs, J. P., Tian, J., and van Norden, S. (2015) "Trend in cycle or cycle in trend? New structural identifications for unobserved-components models of US real GDP." *Macroeconomic Dynamics* **19**, 776-790.

Durbin, J. and Koopman, S. J. (2012) *Time Series Analysis by State Space Methods*. Oxford: Oxford University Press.

Engler, P., and Tervala, J. (2018) "Hysteresis and fiscal policy." *Journal of Economic Dynamics and Control* **93**, 39-53.

Eo, Y., and Morley, J. (2022) "Why has the US economy stagnated since the Great Recession?" *Review of Economics and Statistics* **104**, 246-258.

Fatás, A., and Singh, S. R. (2022). "Supply or demand? Policy makers' confusion in the presence of hysteresis." *Centre for Economic Policy Research (CEPR) Discussion Paper* **DP17232**.

Fernald, J. G., Hall, R. E., Stock, J. H. and Watson, M. W. (2017). "The disappointing recovery of output after 2009." *National Bureau of Economic Research (NBER) Working Paper* **23543**.

Fisher, L. A., Huh, H.-S. and Pagan, A. R. (2016). "Econometric methods for modelling systems with a mixture of I(1) and I(0) variables." *Journal of Applied Econometrics* **31**, 892-911.

Forni, M., Hallin, M., Lippi, M., and Reichlin, L. (2000). "The generalized dynamic-factor model: Identification and estimation." *Review of Economics and Statistics* **82**, 540-554.

Furlanetto, F., Lepetit, A., Robstad, Ø., Rubio-Ramírez, J., and Ulvedal, P. (2021). "Estimating hysteresis effects." *Norges Bank Research Working Paper* **2020-13**.

Galí, J. (2022) "Insider-outsider labor markets, hysteresis and monetary policy." *Journal of Money, Credit and Banking*, **54**, 53-88.

Garga, V. and Singh, S. R. (2021) "Output hysteresis and optimal monetary policy." *Journal of Monetary Economics* **117**, 871-886.

González-Astudillo, M. and Roberts, J. M. (2022) "When are trend-cycle decompositions of GDP reliable?" *Empirical Economics* **62**, 2417-2460.

Gordon, R. J. (2015) "Secular stagnation: A supply-side view." *American Economic Review* **105**, 54-59.

Grant, A. L. and Chan, J. C. (2017) "A Bayesian Model Comparison for Trend-Cycle Decompositions of Output." *Journal of Money, Credit and Banking* **49**, 525-552.

Gyomai, G., and Wildi, M. (2013) "OECD Composite Leading Indicators for G7 Countries: A Comparison of the Hodrick-Prescott Filter and the Multivariate Direct Filter Approach." *OECD Statistics Working Papers* **2012-5**.

Hamilton, J. D. (1989) "A new approach to the economic analysis of nonstationary time series and the business cycle." *Econometrica* **57**, 357-384.

Harvey, A. C. and Shephard, N. (1993) "Structural time series models." In Maddala, G. S., Rao, C. R., and Vinod, H. D. (Eds.) *Handbook of Statistics* **11**, 261-302.

Hasenzagl, T., Pellegrino, F., Reichlin, L., and Ricco, G. (2022) "A Model of the Fed's view on inflation." *Review of Economics and Statistics* **104**, 686-704.

Herrendorf, B., Rogerson, R., and Valentinyi, Á. (2014) "Growth and structural transformation." In Aghion, P. and Durlauf, S. (eds.) *Handbook of Economic Growth.* **Vol. 2B**. Amsterdam: North Holland, pp. 855-941.

Hotta, L. K. (1989) "Identification of unobserved components models." *Journal of Time Series Analysis* **10**, 259-270.

Johnson, K. W., and Li, G. (2010) "The debt-payment-to-income ratio as an indicator of borrowing constraints: Evidence from two household surveys." *Journal of Money, Credit and Banking* **42**, 1373-1390.

Kass, R. E., and Raftery, A. E. (1995) "Bayes factors." *Journal of the American Statistical Association* **90**, 773-795.

Keating, J. W. and Nye, J. V. (1998) "Permanent and transitory shocks in real output: Estimates from nineteenth century and postwar economies." *Journal of Money, Credit and Banking* **30**, 231-251.

Keating, J. (2013a) "What do we learn from Blanchard and Quah decompositions of output if aggregate demand may not be long-run neutral?" *Journal of Macroeconomics* **38**, 203-217.

Keating, J. (2013b) "Interpreting permanent shocks to output when aggregate demand may not be neutral in the long run." *Journal of Money, Credit and Banking* **45**, 747-756.

Keating, J. and Valcarcel, V. J. (2013b) "The time-varying effects of permanent and transitory shocks to real output." *Macroeconomic Dynamics* **19**, 477-507.

Kim, C. J. (1994) "Dynamic linear models with Markov-switching." *Journal of Econometrics* **60**, 1-22.

Li, M. and Mendieta-Muñoz, I. (2020) "Are long-run output growth rates falling?" *Metroeconomica* **71**, 204-234.

Li, M. and Mendieta-Muñoz, I. (2022) "Bayesian analysis of structural correlated unobserved components models and identification via heteroskedasticity." *Studies in Nonlinear Dynamics and Econometrics* **26**, 477-507.

Maffei-Faccioli, N., (2021). "Identifying the sources of the slowdown in growth: Demand vs. supply." *Norges Bank Research Working Paper* **2021-9**.

Mendieta-Muñoz, I. (2017) "On the interaction between economic growth and business cycles." *Macroeconomic Dynamics* **21**, 982-1022.

Mendieta-Muñoz, I. (2018) "The dynamic effects of aggregate supply and demand shocks in the Mexican economy." *Economics Bulletin* **38**, 1-12.

Mitra, S. and Sinclair, T. M. (2012) "Output fluctuations in the G-7: An unobserved components approach." *Macroeconomic Dynamics* **16**, 396-422.

Morley, J. C., Nelson, C. R., and Zivot, E. (2003). "Why are the Beveridge-Nelson and unobserved-components decompositions of GDP so different?" *Review of Economics and Statistics* **85**, 235-243.

Morley, J. C. (2007) "The slow adjustment of aggregate consumption to permanent income." *Journal of Money, Credit and Banking* **39**, 615-638.

Pagan, A., and Robinson, T. (2022) "Excess shocks can limit the economic interpretation." *European Economic Review* **145**, 104-120.

Proietti, T. (2006) "Trend-cycle decompositions with correlated components." *Econometric Reviews* **25**, 61-84.

Sinclair, T. M. (2009) "The relationships between permanent and transitory movements in US output and the unemployment rate." *Journal of Money, Credit and Banking* **41**, 529-542.

Stock, J. and Watson, M. (1988) "Variable trends in economic time series." *Journal of Economic Perspectives* **2**, 147-174.

Tervala, J. (2021) "Hysteresis and the welfare costs of recessions." *Economic Modelling* **95**, 136-144.

Tervala, J. and Watson, T. (2022) "Hysteresis and fiscal stimulus in a recession." *Journal of International Money and Finance* **124**, 102614.

Teulings, C. and Zubanov, N. (2014) "Is economic recovery a myth? Robust estimation of impulse responses." *Journal of Applied Econometrics* **29**, 497-514.

Weber, E. (2011) "Money and economic growth." *Journal of Money, Credit and Banking* **43**, 1579-1597.

Yellen, J. L. (2016) "Macroeconomic research after the crisis." Speech at Conference: *The Elusive 'Great' Recovery: Causes and Implications for Future Business Cycle Dynamics*. 60th Annual Economic Conference Sponsored by the Federal Reserve Bank of Boston (Boston, Massachusetts).

Dynamic hysteresis effects: Online appendix

Mengheng Li*

Ivan Mendieta-Muñoz†

January 4, 2024

This online appendix accompanies: Li, Mengheng and Mendieta-Muñoz, Ivan (2024) "*Dynamic hysteresis effects*". Section 1 provides additional details regarding the Bayesian sampling estimation procedure for parameters and states for the different model's variants. Section 2 presents a small Monte Carlo study. Section 3 provides estimation results that complement the main text, including additional empirical results and a summary of the mixing property of the Markov chain. Section 4 offers details on the computation of the integrated likelihood for the model's variants. This appendix provides only supporting materials and it is not meant for publication. Notations follow the main text, unless stated otherwise.

Keywords: hysteresis; time-to-build effect; trends and cycles; permanent and transitory shocks; state space models; unobserved components.

JEL Classification: C11; C32; E10; E32; O40.

*Senior Lecturer (Assistant Professor). University of Technology Sydney (UTS) Business School and Centre for Applied Macroeconomic Analysis (CAMA). Email: mengheng.li@uts.edu.au

†Associate Professor. Department of Economics, University of Utah. Email: ivan.mendietamunoz@utah.edu

1 Detailed sampling procedure

1.1 Sample $\boldsymbol{\tau}, \boldsymbol{c}|\boldsymbol{y}, \boldsymbol{\theta}$ in the HCUC model

The leftmost matrix in equation (11) of the main text is invertible. This is so because $\boldsymbol{H}_1$ and $\boldsymbol{H}_\phi$ are invertible. By multiplying the inverse of the matrix on both sides and using the block inversion formula we get

$$\begin{pmatrix} \boldsymbol{\tau} \\ \boldsymbol{c} \end{pmatrix} \Bigg| \boldsymbol{\theta} \sim N\left(\begin{bmatrix} \tilde{\boldsymbol{\alpha}} \\ \mathbf{0} \end{bmatrix}, \begin{bmatrix} \boldsymbol{\Omega}_{\boldsymbol{\tau}} & \boldsymbol{\Omega}_{\boldsymbol{\tau c}} \\ \boldsymbol{\Omega}'_{\boldsymbol{\tau c}} & \boldsymbol{\Omega}_{\boldsymbol{c}} \end{bmatrix} \right), \tag{1}$$

where $\tilde{\boldsymbol{\alpha}} = \boldsymbol{H}_1^{-1}\boldsymbol{\alpha}$ and

$$\begin{aligned}
\boldsymbol{\Omega}_{\boldsymbol{\tau}} &= \sigma_\eta^2(\boldsymbol{H}_1'\boldsymbol{H}_1)^{-1} - \rho\sigma_\eta\sigma_\epsilon\big(\boldsymbol{H}_1^{-1}\boldsymbol{H}_\beta(\boldsymbol{H}_1'\boldsymbol{H}_\phi)^{-1} + (\boldsymbol{H}_\phi'\boldsymbol{H}_1)^{-1}(\boldsymbol{H}_1^{-1}\boldsymbol{H}_\beta)'\big) \\
&\quad + \sigma_\epsilon^2\boldsymbol{H}_1^{-1}\boldsymbol{H}_\beta(\boldsymbol{H}_\phi'\boldsymbol{H}_\phi)^{-1}(\boldsymbol{H}_1^{-1}\boldsymbol{H}_\beta)', \\
\boldsymbol{\Omega}_{\boldsymbol{\tau c}} &= \rho\sigma_\eta\sigma_\epsilon(\boldsymbol{H}_\phi'\boldsymbol{H}_1)^{-1} - \sigma_\epsilon^2\boldsymbol{H}_1^{-1}\boldsymbol{H}_\beta(\boldsymbol{H}_\phi'\boldsymbol{H}_\phi)^{-1}, \\
\boldsymbol{\Omega}_{\boldsymbol{c}} &= \sigma_\epsilon^2(\boldsymbol{H}_\phi'\boldsymbol{H}_\phi)^{-1}.
\end{aligned}$$

Considering a multivariate normal distribution, the prior distribution of $\boldsymbol{c}|\boldsymbol{\theta}$ is its marginal distribution given by $N(\mathbf{0}, \boldsymbol{\Omega}_{\boldsymbol{c}}) = N(\mathbf{0}, \sigma_\epsilon^{-2}(\boldsymbol{H}_\phi'\boldsymbol{H}_\phi)^{-1})$. Using standard properties of the multivariate Gaussian distribution, it follows immediately that

$$\boldsymbol{\tau}|\boldsymbol{c}, \boldsymbol{\theta} \sim N\big(\tilde{\boldsymbol{\alpha}} + \boldsymbol{\Omega}_{\boldsymbol{\tau c}}\boldsymbol{\Omega}_{\boldsymbol{c}}^{-1}\boldsymbol{c}, \boldsymbol{\Omega}_{\boldsymbol{\tau}} - \boldsymbol{\Omega}_{\boldsymbol{\tau c}}\boldsymbol{\Omega}_{\boldsymbol{c}}^{-1}\boldsymbol{\Omega}'_{\boldsymbol{\tau c}}\big).$$

Using $\boldsymbol{y}|\boldsymbol{c} = \boldsymbol{\tau}|\boldsymbol{c} + \boldsymbol{c}$, we get $\boldsymbol{y}|\boldsymbol{c}, \boldsymbol{\theta} \sim N\left(\boldsymbol{H}_1^{-1}\boldsymbol{\alpha} + \boldsymbol{H}_1^{-1}\boldsymbol{B}\boldsymbol{c}, (1-\rho^2)\sigma_\eta^2(\boldsymbol{H}_1'\boldsymbol{H}_1)^{-1}\right)$ with $\boldsymbol{B} = \frac{\rho\sigma_\eta}{\sigma_\epsilon}(\boldsymbol{H}_\phi - \boldsymbol{H}_\beta) + \boldsymbol{H}_1$, as shown in the main text. The conditional likelihood also follows immediately.

1.2 Sample $\boldsymbol{\phi}|\boldsymbol{y}, \boldsymbol{c}, \boldsymbol{\delta}, \boldsymbol{\sigma}$ in the HCUC model

The parameter $\boldsymbol{\phi}$ enters the model only by affecting the dynamics of c_t, *i.e.*, $\boldsymbol{H}_\phi\boldsymbol{c} = \boldsymbol{\epsilon}$. We write this as

$$\boldsymbol{c} = \boldsymbol{C}\boldsymbol{\phi} + \boldsymbol{\epsilon}, \tag{2}$$

which is a regression in $\boldsymbol{\phi}$ with a $T \times p$ design matrix $\boldsymbol{C}$ whose i-th column is $(c_{1-i}, ..., c_{T-i})'$, $i = 1, ..., p$. From equation (1), we have:

$$\boldsymbol{\epsilon}|\boldsymbol{y}, \boldsymbol{c}, \boldsymbol{\delta}, \boldsymbol{\sigma} \sim N\left(\boldsymbol{b}, (1-\rho^2)\sigma_\epsilon^2 \boldsymbol{I}_T\right), \quad \boldsymbol{b} = \frac{\rho\sigma_\epsilon}{\sigma_\eta}(\boldsymbol{H}_1\boldsymbol{y} + (\boldsymbol{H}_\beta - \boldsymbol{H}_1)\boldsymbol{c} - \boldsymbol{\alpha}).$$

Given the prior $p(\boldsymbol{\phi})$ specified in the main text, standard Bayesian regression results yield:

$$\boldsymbol{\phi}|\boldsymbol{y}, \boldsymbol{c}, \boldsymbol{\delta}, \boldsymbol{\sigma} \sim N\left(\boldsymbol{K}_{\boldsymbol{\phi}}^{-1}\left(\boldsymbol{\mu}^{\phi} + \frac{1}{(1-\rho^2)\sigma_\epsilon^2}\boldsymbol{C}'(\boldsymbol{c} - \boldsymbol{b})\right), \boldsymbol{K}_{\boldsymbol{\phi}}^{-1}\right) \mathbb{1}_{\{\bar{\lambda}(\boldsymbol{\Phi})<1\}},$$

where $\boldsymbol{K}_{\boldsymbol{\phi}} = \boldsymbol{I}_T + \frac{1}{(1-\rho^2)\sigma_\epsilon^2}\boldsymbol{C}'\boldsymbol{C}$. The necessary truncation within the stationary region is obtained by the acceptance-rejection method.

1.3 Sample $\boldsymbol{\delta}|\boldsymbol{y}, \boldsymbol{c}, \boldsymbol{\phi}, \boldsymbol{\sigma}$ in the HCUC model

Let $-\boldsymbol{H}_\beta \boldsymbol{c}$ be written as $\boldsymbol{\Gamma}\boldsymbol{\beta}$, where $\boldsymbol{\Gamma}$ is a $T \times k$ matrix whose i-th column, $i = 1, ..., k$, is given by $(\boldsymbol{0}_{1\times i}, \mathbb{1}_{\{1\in R\}}c_1, ..., \mathbb{1}_{\{T-i\in R\}}c_{T-i,})'$. From equations (5) and (11) in the main text we have:

$$\boldsymbol{H}_1\boldsymbol{\tau} = \boldsymbol{l}_0\tau_0 + \boldsymbol{l}_1\mu_1 + \boldsymbol{l}_1\mu_2 + \boldsymbol{\Gamma}\boldsymbol{\beta} + \boldsymbol{\eta} = \boldsymbol{X}\boldsymbol{\delta} + \boldsymbol{\eta}, \tag{3}$$

where $\boldsymbol{X} = (\boldsymbol{l}_0, \boldsymbol{l}_1, \boldsymbol{l}_2, \boldsymbol{\Gamma})$ with $\boldsymbol{l}_0 = \left(1, \boldsymbol{0}_{1\times(T-1)}\right)'$, $\boldsymbol{l}_1 = \left(\boldsymbol{1}_{1\times(t_0-1)}, \boldsymbol{0}_{1\times(T-t_0+1)}\right)'$, $\boldsymbol{l}_2 = \boldsymbol{1}_{T\times 1} - \boldsymbol{l}_1$. From (1), $\boldsymbol{\eta}|\boldsymbol{y}, \boldsymbol{\tau}, \boldsymbol{\phi}, \boldsymbol{\sigma} \sim N(\rho\sigma_\eta \boldsymbol{H}_\phi \boldsymbol{c}/\sigma_\epsilon, (1-\rho^2)\sigma_\eta^2 \boldsymbol{I}_T)$. Given the prior $p(\boldsymbol{\delta})$ in the main text, standard Bayesian regression results yield:

$$\boldsymbol{\delta}|\boldsymbol{y}, \boldsymbol{c}, \boldsymbol{\phi}, \boldsymbol{\sigma} \sim N\left(\boldsymbol{K}_\delta^{-1}\left((\boldsymbol{V}^\delta)^{-1}\boldsymbol{\mu}^\delta + \frac{1}{(1-\rho^2)\sigma_\eta^2}\boldsymbol{X}'\left(\boldsymbol{H}_1\boldsymbol{\tau} - \frac{\rho\sigma_\eta}{\sigma_\epsilon}\boldsymbol{H}_\phi\boldsymbol{c}\right)\right), \boldsymbol{K}_\delta^{-1}\right),$$

where $\boldsymbol{K}_\delta = (\boldsymbol{V}^\delta)^{-1} + \frac{1}{(1-\rho^2)\sigma_\eta^2}\boldsymbol{X}'\boldsymbol{X}$.

1.4 Sample $\boldsymbol{\sigma}|\boldsymbol{y}, \boldsymbol{c}, \boldsymbol{\delta}, \boldsymbol{\phi}$ in the HCUC model

Notice that $\boldsymbol{\eta} = \boldsymbol{H}_1\boldsymbol{\tau} + \boldsymbol{H}_\beta\boldsymbol{c} - \boldsymbol{\alpha}$ and $\boldsymbol{\epsilon} = \boldsymbol{H}_\phi\boldsymbol{c}$. The conditional likelihood of $\boldsymbol{\zeta} = (\boldsymbol{\eta}', \boldsymbol{\epsilon}')'$ is similar to the one in the CUC model studied by Grant and Chan (2017). We first derive the

density of $\boldsymbol{\zeta}$. By completing the square, equation (4) in the main text implies

$$p(\boldsymbol{\zeta}|\boldsymbol{\sigma}) \propto (\sigma_\epsilon^2)^{-\frac{T}{2}} \exp\left(-\frac{1}{2\sigma_\epsilon^2}\sum_{t=1}^{T}\epsilon_t^2\right)\left((1-\rho^2)\sigma_\eta^2\right)^{-\frac{T}{2}} \exp\left(-\frac{1}{2(1-\rho^2)\sigma_\eta^2}\sum_{t=1}^{T}\left(\eta_t - \frac{\rho\sigma_\eta}{\sigma_\epsilon}\epsilon_t\right)^2\right)$$
$$\propto \left((1-\rho^2)\sigma_\eta^2\sigma_\epsilon^2\right)^{-\frac{T}{2}} \exp\left(-\frac{1}{2\sigma_\epsilon^2}z_3 - \frac{1}{2(1-\rho^2)\sigma_\eta^2}\left(z_1 - \frac{2\rho\sigma_\eta}{\sigma_\epsilon}z_2 + \frac{\rho^2\sigma_\eta^2}{\sigma_\epsilon^2}z_3\right)\right), \tag{4}$$

where $z_1 = \boldsymbol{\eta}'\boldsymbol{\eta}$, $z_2 = \boldsymbol{\eta}'\boldsymbol{\epsilon}$, and $z_3 = \boldsymbol{\epsilon}'\boldsymbol{\epsilon}$.

On the other hand, $p(\boldsymbol{\zeta}|\boldsymbol{\sigma})$ in (4) can be used to factorize the conditional posteriors of σ_ϵ^2, σ_η^2, and ρ. Considering the uniform priors used for these parameters in the main text, the posterior is proportional to the respective likelihood. Let $\boldsymbol{A}/a$ for $a \in \boldsymbol{A}$ denote the the complement of a in $\boldsymbol{A}$. We have:

$$p(\sigma_\eta^2|\boldsymbol{y}, \boldsymbol{c}, \sigma_\epsilon^2, \rho) \propto (\sigma_\eta^2)^{-\frac{T}{2}} \exp\left(-\frac{1}{2(1-\rho^2)\sigma_\eta^2}\left(z_1 - \frac{2\rho\sigma_\eta}{\sigma_\epsilon}z_2 + \frac{\rho^2\sigma_\eta^2}{\sigma_\epsilon^2}z_3\right)\right),$$
$$p(\sigma_\epsilon^2|\boldsymbol{y}, \boldsymbol{c}, \sigma_\eta^2, \rho) \propto (\sigma_\epsilon^2)^{-\frac{T}{2}} \exp\left(-\frac{1}{2\sigma_\epsilon^2}z_3 - \frac{1}{2(1-\rho^2)\sigma_\eta^2}\left(z_1 - \frac{2\rho\sigma_\eta}{\sigma_\epsilon}z_2 + \frac{\rho^2\sigma_\eta^2}{\sigma_\epsilon^2}z_3\right)\right),$$
$$p(\rho|\boldsymbol{y}, \boldsymbol{c}, \sigma_\epsilon^2, \sigma_\eta^2) \propto (1-\rho^2)^{-\frac{T}{2}} \exp\left(-\frac{1}{2(1-\rho^2)\sigma_\eta^2}\left(z_1 - \frac{2\rho\sigma_\eta}{\sigma_\epsilon}z_2 + \frac{\rho^2\sigma_\eta^2}{\sigma_\epsilon^2}z_3\right)\right).$$

This step is implemented by a simple Griddy-Gibbs step: we use a fine grid defined by the bounds of the uniform prior to evaluate and normalize the above expressions into empirical cumulative distribution functions (cdf). With a draw from $U(0,1)$, we then choose the largest grid point whose empirical cdf is smaller than the draw—that is, the inverse-transform method.

1.5 Sample $s|\boldsymbol{y}, \boldsymbol{c}, \boldsymbol{\delta}, \boldsymbol{\phi}, \boldsymbol{\sigma}, q$ in the H^{s}CUC model

Let $s_t \in \{1, 0\}$ denote the state at t that indicates if hysteresis effect is active, for $t = 1, ..., T$. We design a single-move sampler for posterior computation. By combining (2) and equation (4) in the main text we have:

$$\boldsymbol{\epsilon} = \boldsymbol{c} - \boldsymbol{C}\boldsymbol{\phi}, \quad \eta_t|\boldsymbol{c}, \boldsymbol{\sigma} \sim N\left(\frac{\rho\sigma_\eta}{\sigma_\epsilon}\epsilon_t, (1-\rho^2)\sigma_\eta^2\right).$$

Using the result above and (3), conditional on $\boldsymbol{y}$, $\boldsymbol{c}$, $\boldsymbol{\delta}$, $\boldsymbol{\phi}$, and $\boldsymbol{\sigma}$ we have

$$\boldsymbol{y}^* = \boldsymbol{S}\boldsymbol{c} + \boldsymbol{\eta}^*, \quad \boldsymbol{\eta}^* \sim N(\boldsymbol{0}, (1-\rho^2)\sigma_\eta^2\boldsymbol{I}_T), \tag{5}$$

where $\boldsymbol{y}^* = \boldsymbol{H}_1(\boldsymbol{y} - \boldsymbol{c}) - \boldsymbol{l}_0\tau_0 - \boldsymbol{l}_1\mu_1 - \boldsymbol{l}_1\mu_2 - \frac{\rho\sigma_\eta}{\sigma_\epsilon}(\boldsymbol{c} - \boldsymbol{C}\boldsymbol{\phi})$, and $\boldsymbol{S}$ is a $T \times T$ matrix whose t-th row takes the form

$$\begin{bmatrix}\boldsymbol{0}_{1\times(t-k-1)} & s_{t-k}\beta_k & \dots & s_{t-2}\beta_2 & s_{t-1}\beta_1 & \boldsymbol{0}_{1\times(T-t+1)}\end{bmatrix}.$$

Notice two important results: (i) the first row of $\boldsymbol{S}$ contains only zeros since the hysteresis effect means that the cycle should affect the trend with lags, indicating that only s_1, ..., s_{T-1} are identifiable; and (ii) s_t only enters the likelihood of y^*_{t+1}, ..., y^*_{t+k} in (5) (with the obvious simplification for s_t with $t > T - k$). For example, with $k = 3$, we have

$$\begin{aligned}
y_2^* &= s_1\beta_1 c_1 + 0 + 0 + 0 + \eta_2^*,\\
y_3^* &= s_1\beta_2 c_1 + s_2\beta_1 c_2 + 0 + 0 + \eta_3^*,\\
y_4^* &= s_1\beta_3 c_1 + s_2\beta_2 c_2 + s_3\beta_1 c_3 + 0 + \eta_4^*,\\
y_5^* &= 0 + s_2\beta_3 c_2 + s_3\beta_2 c_3 + s_4\beta_1 c_4 + \eta_5^*.
\end{aligned}$$

This observation facilitates a single-move sampler that recursively computes

$$p(\boldsymbol{s}|\boldsymbol{y}, \boldsymbol{c}, \boldsymbol{\delta}, \boldsymbol{\phi}, \boldsymbol{\sigma}, \boldsymbol{q}) \propto p(\boldsymbol{y}^*|\boldsymbol{s}, \boldsymbol{c}, \boldsymbol{\sigma})p(\boldsymbol{s}|\boldsymbol{q})$$

via the factorization

$$p(s_t|\boldsymbol{y}, \boldsymbol{c}, \boldsymbol{\delta}, \boldsymbol{\phi}, \boldsymbol{\sigma}, \boldsymbol{q}, \boldsymbol{s}/s_t) \propto p(y^*_{t+1}, ..., y^*_{t+k}|s_t, c_{t-k+2}, ..., c_{t+k-1}, \boldsymbol{\sigma})p(s_{t+1}|s_t, \boldsymbol{q})p(s_t|s_{t-1}, \boldsymbol{q}),$$

where $\boldsymbol{q} = (q_{00}, q_{11})'$ defines the transition probability of the Markov process s_t. The likelihood—that is, the first term on the right-hand side—is Gaussian and given by

$$y^*_{t+1}, ..., y^*_{t+k}|s_t, c_{t-k+1}, ..., c_{t+k-1}, \boldsymbol{\sigma} \sim N\left(\begin{bmatrix} y^*_{t+1} - \sum_{i=1}^k s_{t-i+1}\beta_i c_{t-i+1} \\ \vdots \\ y^*_{t+k} - \sum_{i=1}^k s_{t-i+k}\beta_i c_{t-i+k}\end{bmatrix}, (1-\rho^2)\sigma_\eta^2 \boldsymbol{I}_k\right).$$

Assuming that the current value in the Markov chain is s_t^{old} (for $\boldsymbol{s}/s_t^{\text{old}}$, we suppress the superscript), we generate a new draw s_t^{new} from $p(s_t|s_{t-1}, \boldsymbol{q})$, that is, a Bernoulli variate. The

acceptance rate is given by:

$$\min\left[\frac{p(y^*_{t+1},...,y^*_{t+k}|s^{\text{new}}_t,c_{t-k+2},...,c_{t+k-1},\boldsymbol{\sigma})p(s_{t+1}|s^{\text{new}}_t,\boldsymbol{q})p(s^{\text{new}}_t|s_{t-1},\boldsymbol{q})p(s^{\text{old}}_t|s_{t-1},\boldsymbol{q})}{p(y^*_{t+1},...,y^*_{t+k}|s^{\text{old}}_t,c_{t-k+2},...,c_{t+k-1},\boldsymbol{\sigma})p(s_{t+1}|s^{\text{old}}_t,\boldsymbol{q})p(s^{\text{old}}_t|s_{t-1},\boldsymbol{q})p(s^{\text{new}}_t|s_{t-1},\boldsymbol{q})},1\right].$$

The above single-move Metropolis-Hastings (MH) algorithm is completed recursively for all t.

1.6 Sample $q|s$ in the H^{s}CUC model

We initialize the Markov regimes by setting $s_t \sim Ber(1-\bar{q}_0)$, where $(\bar{q}_0, 1-\bar{q}_0)'$ denote the stationary distribution of the two-state Markov process s_t. Equivalently, the latter is the eigenvector of $\boldsymbol{Q}'$, where

$$\boldsymbol{Q} = \begin{bmatrix} q_{00} & 1-q_{00} \\ 1-q11 & q_{11} \end{bmatrix}.$$

With this initialization, the Dirichlet distribution is no longer conjugate. This requires a MH step. Specifically, candidate draws q^{new}_{00} and q^{new}_{11} are generated by:

$$(q^{\text{new}}_{00}, 1-q^{\text{new}}_{00})' \sim Dir\left(e_1 + \sum_{t=2}^{T-1}\mathbb{1}_{\{s_{t-1}=0,s_t=0\}}, e_2 + \sum_{t=2}^{T-1}\mathbb{1}_{\{s_{t-1}=0,s_t=1\}}\right),$$
$$(1-q^{\text{new}}_{11}, q^{\text{new}}_{11})' \sim Dir\left(e_2 + \sum_{t=2}^{T-1}\mathbb{1}_{\{s_{t-1}=1,s_t=0\}}, e_1 + \sum_{t=2}^{T-1}\mathbb{1}_{\{s_{t-1}=1,s_t=1\}}\right),$$

respectively. With the candidate draw, we can compute $\bar{q}^{\text{new}}_0$. The draw is then accepted with probability

$$\min\left[\frac{s_1^{1-\bar{q}^{\text{new}}_0}(1-s_1)^{\bar{q}^{\text{new}}_0}}{s_1^{1-\bar{q}^{\text{old}}_0}(1-s_1)^{\bar{q}^{\text{old}}_0}},1\right].$$

2 A small Monte Carlo study

Basistha (2007) and González-Astudillo and Roberts (2022) documented that more precise estimates of the trend-cycle correlation coefficient and a more accurate output gap can be obtained by using a bivariate model. Both Basistha (2007) and González-Astudillo and Roberts (2022) also discussed that a univariate model tends to overestimate the correlation coefficient and attributes more output variation to the trend rather than to the cycle, or $\sigma_\eta > \sigma_\epsilon$, a result also found in Morley et al. (2003) and Grant and Chan (2017).

Following these contributions, we considered a multivariate model and a Bayesian model

averaging exercise in the main text. Our main message in this regard is that this overestimation may be a result of omitting the hysteresis effects, besides the identification issues (which can be mitigated by using multivariate information). Regarding the latter, Oh et al. (2008) showed that there is a set of equivalent UC models, with or without trend-cycle correlation, that yields the same reduced-form ARIMA representation for a univariate time series. The intrinsic tension in terms of identification comes from the MA components in the reduced form (derived from the cycle dynamics) and the correlation term, as we discuss in the main text (see also Trenkler and Weber, 2016 and Li and Mendieta-Muñoz, 2021). The proposed HCUC model is fully identified in the finite sample under the conditions specified in the main text, which are satisfied by the logarithm of US real GDP. Consequently, the overestimation of the correlation coefficient does not represent a problem, as can be observed by the similar results obtained from the multivariate H^{m}CUC model. This result is also supported by Oh et al. (2008)'s result that, when the data generating process (DGP) has zero trend-cycle correlation, both the CUC model and the Beveridge-Nelson decomposition generate an output gap that is fairly similar to the HP-filtered cycle or a standard UC model.

To examine more thoroughly if our baseline HCUC model tends to overestimate ρ, we consider a small Monte Carlo study with several data features that mimic the logarithm of US real GDP. We set $T = 300$ data points (our sample is composed of $T = 303$ quarterly data). We choose $\phi_1 = 1.3$ and $\phi_2 = -0.5$, which implies a periodicity of 3.88 years, *i.e.*, somewhere between the values obtained from the UC model and the CUC model. We modified the following data features:

1. A five-quarters recession occurs every m_i quarters, with $i = 1, 2, 3$ and $m_1 = 5$, $m_2 = 15$, and $m_3 = 25$.

2. $\sigma_\eta = w_i \sigma_\epsilon$, with $\sigma_\epsilon = 0.5$ and $w_1 = 0.5$, $w_2 = 1$, and $w_3 = 5$.

We set $\rho = 0$ throughout the exercise to focus on the overestimation issue, as in Basistha (2007), Oh et al. (2008), and González-Astudillo and Roberts (2022). For each "$m_i + w_j$" combination, we simulate 100 datasets and conducted the estimation following the same algorithm described in the main text. The whole estimation process takes a bit less than 2 hours on a laptop with 24 CPU workers.

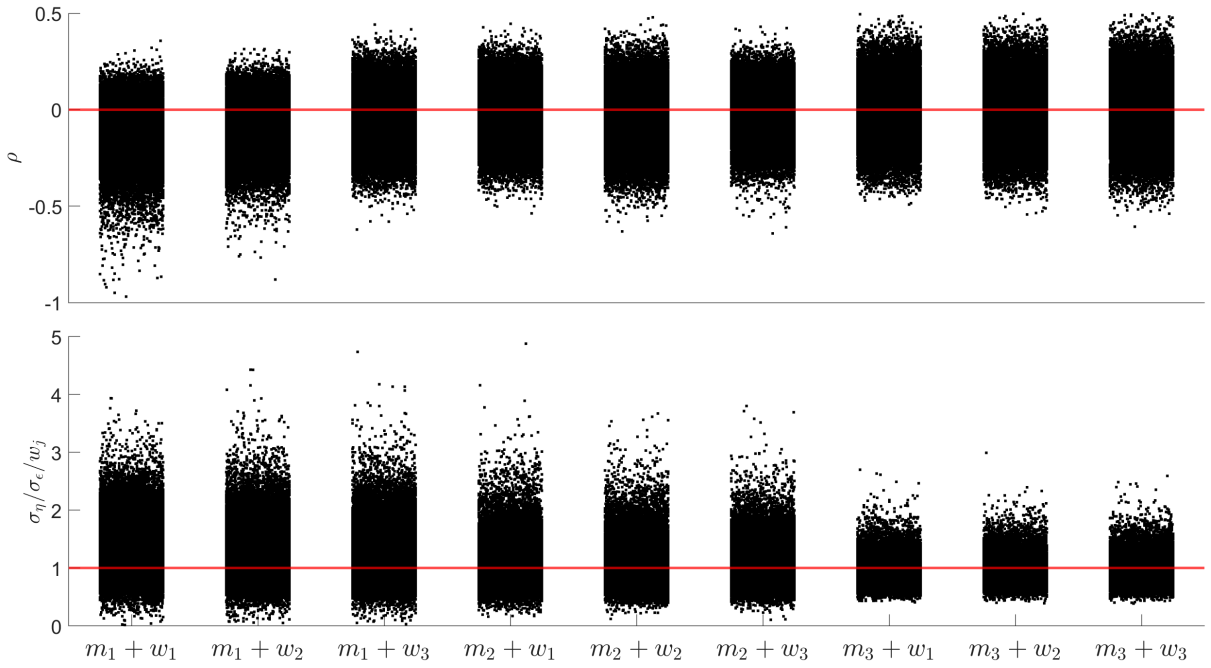

Figure 1: Trend-cycle correlation coefficient (above) and rescaled signal-to-noise ratio (below). Each rectangular cloud plot contains 100 bars, with each bar containing all posterior draws for a simulated dataset. The x-axis shows the $m_i + w_j$ combination, $i, j = 1, 2, 3$, which indicates the Monte Carlo setup. The red line indicates the true DGP value.

As mentioned above, it is often observed that the overestimation of ρ is associated with the tendency to attribute output variation to trend volatility σ_η. Hence, we report all sampled draws of $v = \sigma_\eta/\sigma_\epsilon/w$, where a value close to 1 suggests correct estimation, whereas a value larger than 1 indicates overestimation of trend volatility under the simulation with signal-to-noise ratio w. Figure 1 shows the posterior draws of the trend-cycle correlation ρ and the rescaled signal-to-noise ratio v, relative to their theoretical values.

The figure reveals two interesting results. First, the proposed HCUC model seems to also overestimate ρ, as the CUC model studied by Basistha (2007) and González-Astudillo and Roberts (2022), among others, but only for the case of excessively frequent recessions and low trend volatility. Hence, when the frequency of recessions decreases—that is, when it is closer to the actual frequency of recessions defined by the NBER, the inclusion of the hysteresis effect helps to mitigate the overestimation issue, as found for $m_2 + w_1$ and $m_3 + w_1$. This further supports our finding shown in Figure 4 in the main text.

Second, we notice that σ_η tends to be overestimated when the trend volatility is low, a result also emphasized by Oh et al. (2008) and Grant and Chan (2017). This result suggests that the

"pile-up" problem pointed out by Stock and Watson (1998) is likely due to the omission of trend-cycle correlation. However, a caveat of any CUC model is that the inclusion of such correlation tends to overshoot the trend volatility. Thus, our simulation study makes it clear that, for the HCUC model, the overestimation issue is mainly associated with the frequency of recessions (as seen by the results obtained when m_2 and m_3, compared to ones obtained when m_1). The reason for this is that the dynamic hysteresis effects in the proposed model remain active for 9 quarters, as illustrated in Table 1 of the main text. Yet, with a new recession occurring before the completion of the dynamic hysteresis effect (that is, under m_1), there exists contradicting information that identify the hysteresis effect coefficients. Consequently, the variation in the output gap is underestimated, thus increasing the trend volatility.

In sum, if the frequency of recessions is (unrealistically) high, the proposed HCUC model may run into finite-sample issues if the recession periods or number of activation periods (*i.e.*, the value of k) is not extended accordingly. However, given the much lower frequency of recessions in the US as defined by the NBER, we are confident that our HCUC model provides accurate estimates with sound inference.

3 Additional estimation results

3.1 Complementary empirical results

Figure 2 below shows the cumulative hysteresis effects for all models. Following also the results reported in the main text, the hysteresis effect begins after the early 1970s, with a negative output gap decreasing potential output in recessions.

It may be possible to attribute the absence of positive hysteresis effects after 1970, compared to the "bouncing back" of HE_t observed in Figure 1 of the main text, to the selection of 2 quarters exceeding NBER recessions used in our definition of extended recession periods. To examine the robustness of our results to different definitions of extended recession periods R, we also consider dynamic hysteresis effects estimated from models that incorporate more quarters after the end of the NBER recessions. Results are illustrated in Figure 3. It is clear that the estimated paths of the dynamic hysteresis effect do not alter our conclusion. Together with the results of other variants of the baseline model reported in main text—especially the H^2CUC, H^lCUC, and the H^sCUC models, which also feature hysteresis effects outside R, the figure

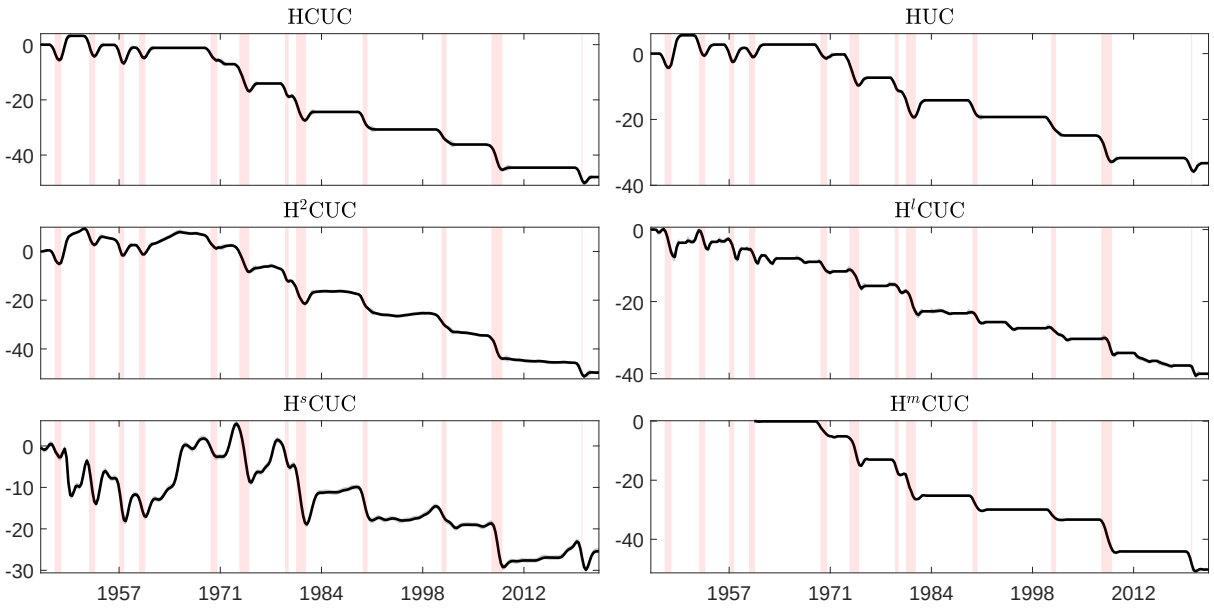

Figure 2: Cumulative hysteresis effect. We report the posterior median and 90% credible intervals of $CHE_t = \sum_{s=1}^{t} HE_s$. CHE_t shows the cumulative permanent loss due to cyclical movements. Shaded areas indicate NBER recession dates.

provides additional evidence supporting the emergence of hysteresis effects after 1970.

Recently, several authors, including Furlanetto et al. (2021) and Benati and Lubik (2022), have also found hysteresis effects that predominantly appear after 1980. Our results provide complementary evidence supporting these studies. Due to the activation and the deactivation of hysteresis effects across time, our HCUC model (and its variants) allows for the hysteresis coefficients, *i.e.* β_i's, to capture various dynamic evolutions, as illustrated in Table 1 in the main text. To examine parameter stability, we follow the literature and conduct different sub-sample robustness checks, using 1970:Q1, 1980:Q1, and 1990:Q1 as cut-off points. Table 1 shows the estimation results. Interestingly, the results corroborate the main results obtained from the model that considered the full sample, as reported in Table 2 of the main text, the only exception being that the pre-1970 sample yields different coefficient estimates. This result echoes with our finding that hysteresis effects took place mainly after 1970—which implies that, before then, negative output hysteresis tended to be compensated by subsequent positive output hysteresis. Overall, the sub-sample checks corroborate that the full-sample hysteresis effects are largely influenced by the post-1970 output dynamics.

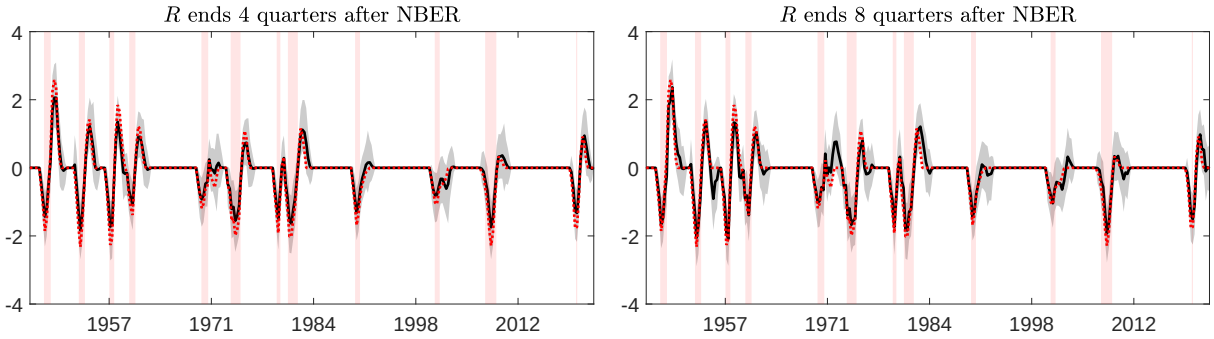

Figure 3: Hysteresis effect with different definitions of R. We report the posterior median and 90% credible intervals of HE_t, estimated using models with the extended recession periods R. The latter were defined as those spanning the NBER recessions but also covering 2 quarters before and 4 quarters (left) or 8 quarters (right) after the end of NBER recessions. The red dotted line indicates the posterior median of HE_t for the HCUC model reported in the main text. Shaded areas indicate NBER recession dates.

Table 1: Hysteresis effect coefficients obtained from the HCUC model for different sub-samples

Cut-off	1970:Q1		1980:Q1		1990:Q1	
	Pre	Post	Pre	Post	Pre	Post
β_1	0.36 (0.28) [−0.08, 0.71]	**0.72** (0.24) [0.44, 1.07]	**0.46** (0.18) [0.26, 0.72]	**0.51** (0.31) [0.19, 0.91]	**0.62** (0.27) [0.39, 0.94]	**0.52** (0.20) [0.34, 0.86]
β_2	**0.23** (0.14) [0.04, 0.41]	**0.38** (0.20) [0.11, 0.62]	**0.37** (0.19) [0.15, 0.66]	**0.41** (0.28) [0.14, 0.76]	**0.55** (0.31) [0.20, 0.93]	**0.48** (0.25) [0.19, 0.74]
β_3	**−0.17** (0.08) [−0.31, −0.03]	**0.46** (0.22) [0.18, 0.83]	**0.33** (0.16) [0.15, 0.77]	**0.82** (0.19) [0.57, 1.01]	**0.50** (0.31) [0.14, 0.96]	**0.76** (0.22) [0.44, 1.08]
β_4	**−0.11** (0.06) [−0.21, 0.00]	−0.04 (0.15) [−0.24, 0.18]	0.10 (0.31) [−0.26, 0.47]	−0.08 (0.24) [−0.37, 0.18]	0.15 (0.47) [−0.40, 0.72]	−0.07 (0.25) [−0.33, 0.20]

Notes: We report the posterior medians, standard deviations in parentheses, and the 90% credible intervals in square brackets. Bold numbers indicate that the respective coefficient's credible interval does not include zero. Three split-sample experiments are conducted with 1970:Q1, 1980:Q1, and 1990:Q1 as the cut-off points, respectively.

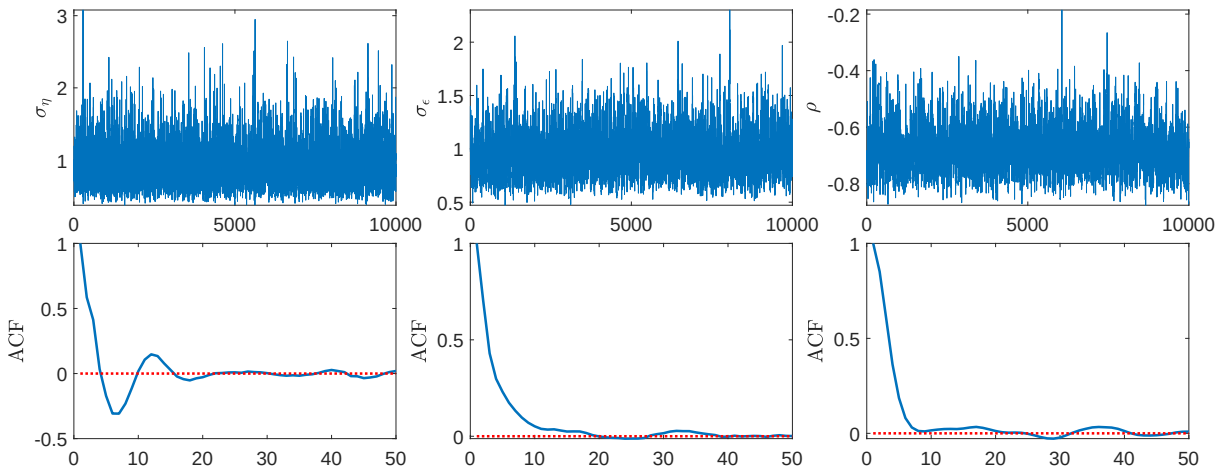

Figure 4: Posterior trace and ACF obtained from the HCUC model. Reported are the posterior traces and ACFs of σ_η, σ_ϵ, and ρ . Both posterior statistics are computed after burn-in and thinning.

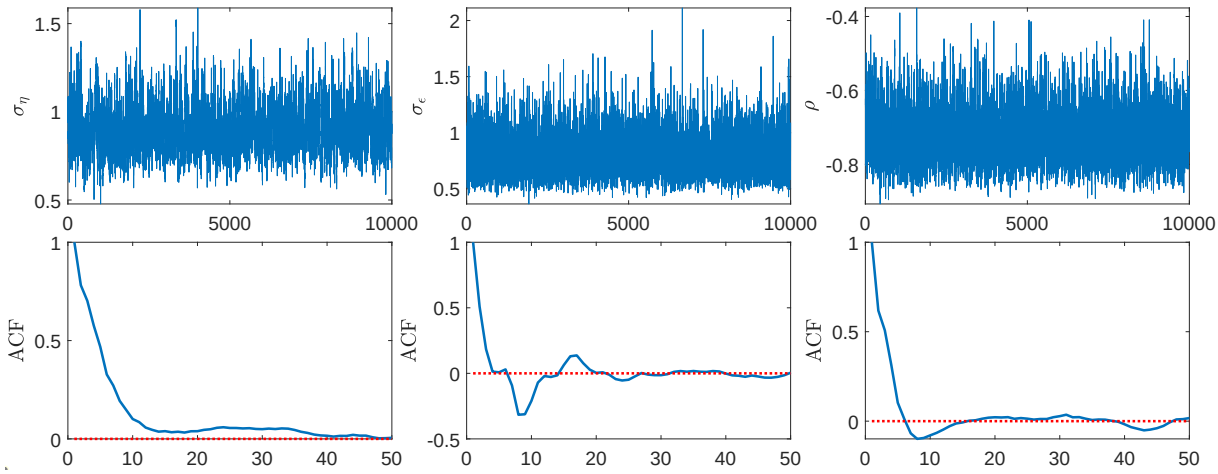

Figure 5: Posterior trace and ACF obtained from the H^2CUC model. Reported are the posterior traces and ACFs of σ_η, σ_ϵ, and ρ. Both posterior statistics are computed after burn-in and thinning.

3.2 Mixing of the Markov chain

To evaluate the mixing property of the MCMC algorithm, we report the posterior trace and autocorrelation function (ACF) of σ_η^2, σ_ϵ^2, and ρ for all models with correlated innovations and dynamic hysteresis effect, after burn-in and thinning. These are reported in figures 4 through 8. We focus on these parameters because they are the least efficiently estimated among all models' parameters.

From the reported ACFs, it can be seen that the mixing of the chain is satisfactory, as shown by the fast decaying patterns. Among all models, the H^sCUC models seems to be the least efficiently estimated; whereas the H^mCUC models appears to show superior mixing efficiency.

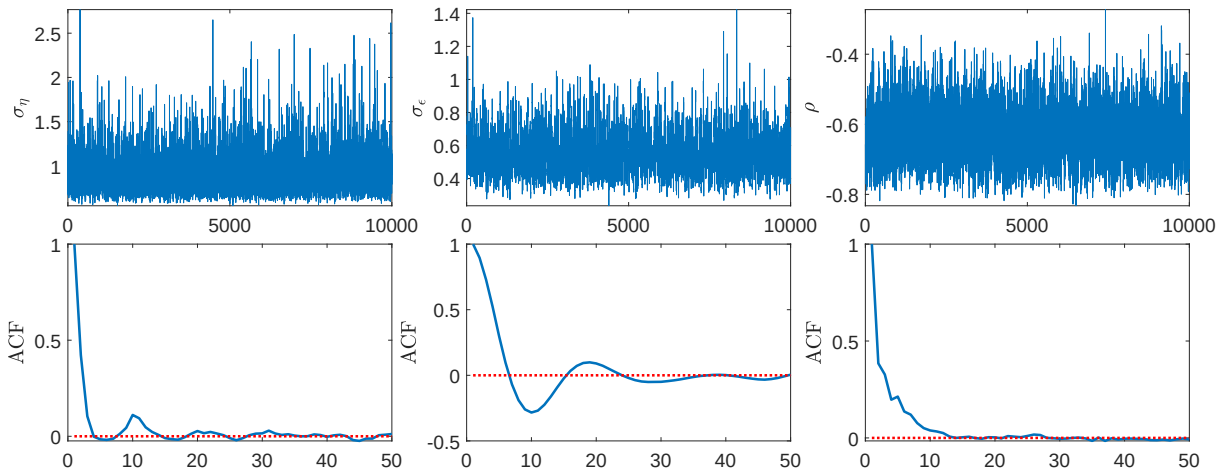

Figure 6: Posterior trace and ACF obtained from the H^{l}CUC model. Reported are the posterior traces and ACFs of σ_η, σ_ϵ, and ρ. Both posterior statistics are computed after burn-in and thinning.

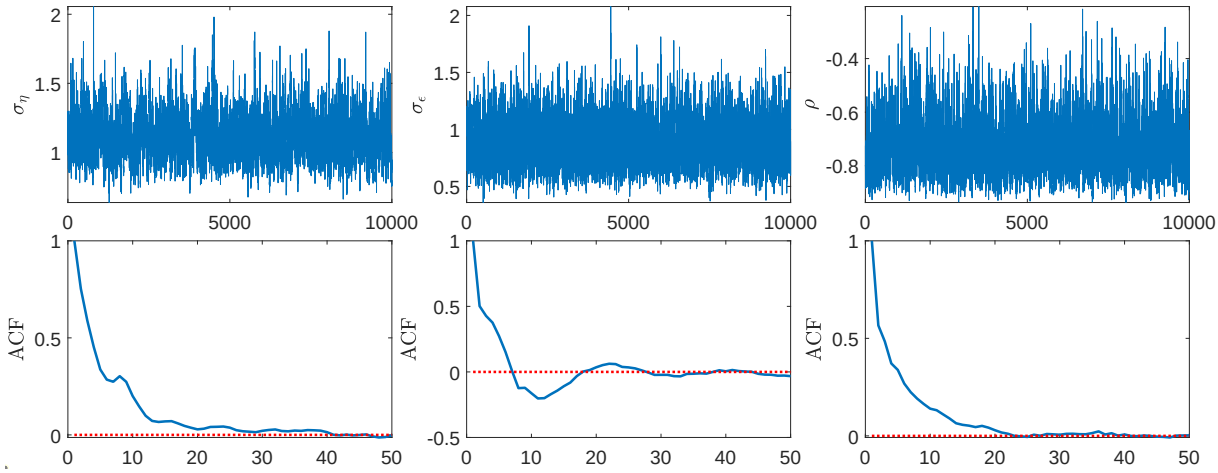

Figure 7: Posterior trace and ACF obtained from the H^{s}CUC model. Reported are the posterior traces and ACFs of σ_η, σ_ϵ, and ρ. Both posterior statistics are computed after burn-in and thinning.

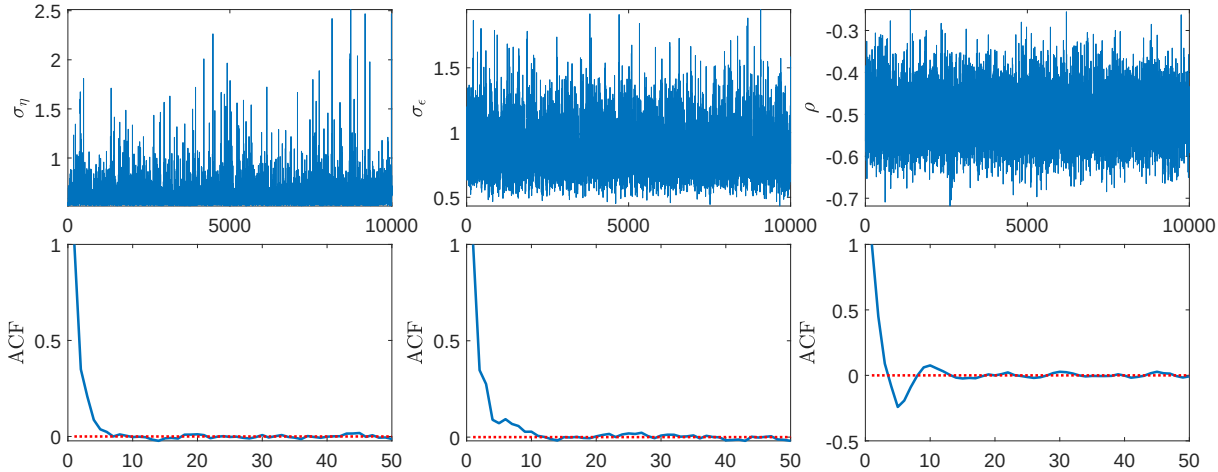

Figure 8: Posterior trace and ACF obtained from the H^{m}CUC model. Reported are the posterior traces and ACFs of σ_η, σ_ϵ, and ρ. Both posterior statistics are computed after burn-in and thinning.

Table 2: Mixing of the Markov chain for the proposed models

	HCUC	H^{2}CUC	H^{l}CUC	H^{s}CUC	H^{m}CUC
	Maximum IEF among model parameters				
τ_0	3.72	4.20	4.46	8.34	3.55
$\boldsymbol{\mu}$	2.10	3.98	6.51	6.24	2.60
$\boldsymbol{\phi}$	3.43	4.59	2.64	10.57	4.66
σ_η	9.34	8.27	6.48	13.40	3.81
σ_ϵ	9.22	11.52	9.37	16.84	5.07
ρ	7.51	8.65	7.00	13.23	5.02
$\boldsymbol{\beta}$	4.12	4.50	5.33	8.92	6.71
$\{c_t\}$	13.85	11.27	7.06	15.45	8.29
$\{s_t\}$	-	-	-	17.59	-
$\boldsymbol{q}$	-	-	-	12.74	-

Notes: The table summarizes the mixing property of the Markov chain for all models with correlated trend and cycle innovations and hysteresis effect via the maximum IEF among grouped parameters shown on the left column. Results are based on every 5-th draw from the 70,000 MCMC samples with the first 20,000 burn-in periods discarded.

We also report the corresponding inefficiency factor (IEF) in table 2, together with some other relevant models' parameters. The IEF is the number of draws needed to achieve the same inferential accuracy as that of independent draws. Thus, a smaller IEF is preferred, see, *e.g.*, Chib and Greenberg (1995) for an introduction.

Table 2 shows that the static parameters in all models are efficiently estimated, with an implied effective sample size (ESS) larger than 10% of the MCMC sample size (Chib and Greenberg, 1995). The only exception is the H^{s}CUC model, where the maximum IEF of $\boldsymbol{\phi}$ and $\boldsymbol{\sigma}$ is slightly above 10, suggesting a less-than-10% ESS. Given our MCMC sample size of 10,000 after burn-in and thinning, the posterior distribution of σ_ϵ (the one with the largest IEF) is still composed of more than 590 effective sample points. Thus, we do not consider this to be a major issue. One potential explanation for this may be associated with the use of a single-move sampler for $\{s_t\}_{t=1}^{\infty}$ and a MH algorithm for $\boldsymbol{q}$ in the H^{s}CUC model. As shown by the inferior IEF for s_t's, the possibly low acceptance rate of s_t^{new} contributes to increased correlation among MCMC samples. However, with an IEF of 17, the ESS amounts to 580, rendering the performance of the developed algorithm acceptable. An interesting future research may look into more efficient algorithms that sample unobserved switching regimes in the UC framework, where switching dynamics similar to the ones proposed in the main text are more complex than the Markov switching state space models studied by Kim (1994).

4 Integrated likelihood

4.1 Integrated likelihood for the HCUC, the H^{2}CUC, and the H^{l}CUC models

The integrated likelihood can be derived by completing the square. Let us denote $k = \left(2\pi\sigma_\eta^2\sigma_\epsilon^2(1-\rho^2)\right)^{-\frac{T}{2}}$ for each specific model. For instance, using equations (13) and (14) in the main text, we have the following for the HCUC model:

$$\begin{aligned}
p(\boldsymbol{y}|\boldsymbol{\theta}) &= k\int \exp\left(-\frac{1}{2(1-\rho^2)\sigma_\eta^2}(\boldsymbol{H}_1\boldsymbol{y}-\boldsymbol{\alpha}-\boldsymbol{B}\boldsymbol{c})'(\boldsymbol{H}_1\boldsymbol{y}-\boldsymbol{\alpha}-\boldsymbol{B}\boldsymbol{c})\right)\exp\left(-\frac{1}{2\sigma_\epsilon^2}\boldsymbol{c}'\boldsymbol{H}_\phi'\boldsymbol{H}_\phi\boldsymbol{c}\right)d\boldsymbol{c}\\
&= k\exp\left(-\frac{1}{2}\left[\frac{1}{(1-\rho^2)\sigma_\eta^2}(\boldsymbol{H}_1\boldsymbol{y}-\boldsymbol{\alpha})'(\boldsymbol{H}_1\boldsymbol{y}-\boldsymbol{\alpha})-\boldsymbol{b}_{\boldsymbol{c}}'\boldsymbol{K}_{\boldsymbol{c}}^{-1}\boldsymbol{b}_{\boldsymbol{c}}\right]\right)\\
&\quad\times\int\exp\left(-\frac{1}{2}(\boldsymbol{c}-\boldsymbol{K}_{\boldsymbol{c}}^{-1}\boldsymbol{b}_{\boldsymbol{c}})'\boldsymbol{K}_{\boldsymbol{c}}(\boldsymbol{c}-\boldsymbol{K}_{\boldsymbol{c}}^{-1}\boldsymbol{b}_{\boldsymbol{c}})\right)d\boldsymbol{c}\\
&= k\left|\boldsymbol{K}_{\boldsymbol{c}}\right|^{-\frac{1}{2}}\exp\left(-\frac{1}{2}\left[\frac{1}{(1-\rho^2)\sigma_\eta^2}(\boldsymbol{H}_1\boldsymbol{y}-\boldsymbol{\alpha})'(\boldsymbol{H}_1\boldsymbol{y}-\boldsymbol{\alpha})-\boldsymbol{b}_{\boldsymbol{c}}'\boldsymbol{K}_{\boldsymbol{c}}^{-1}\boldsymbol{b}_{\boldsymbol{c}}\right]\right),
\end{aligned}$$

where $\boldsymbol{b}_{\boldsymbol{c}} = (\sigma_\eta^2-\rho^2\sigma_\eta^2)^{-1}\boldsymbol{B}'(\boldsymbol{H}_1\boldsymbol{y}-\boldsymbol{\alpha})$; and $\boldsymbol{B}$ and $\boldsymbol{K}_{\boldsymbol{c}}$ are the sparse band matrices defined in the main text. The marginal data likelihoods for the other univariate and linear model's variants can be constructed in an identical way.

4.2 Integrated likelihood for the H^{s}CUC model

Notice that the H^{s}CUC model is conditionally linear and Gaussian: given s_t, $t = 1, ..., T-1$, the model is linear and Gaussian. Thus, it can be handled by using the Kalman filer to integrate out the trend or the cycle. In other words, in the integrated likelihood

$$p(\boldsymbol{y}|\boldsymbol{\theta}) = \int\int p(\boldsymbol{y},\boldsymbol{c}|\boldsymbol{\theta},\boldsymbol{s})p(\boldsymbol{s}|\boldsymbol{\theta})d\boldsymbol{c}d\boldsymbol{s},$$

the inner integrand $p(\boldsymbol{y},\boldsymbol{c}|\boldsymbol{\theta},\boldsymbol{s})$ can be computed using prediction error decomposition via the Kalman filter. Suppressing the dependence on the static parameter vector $\boldsymbol{\theta}$, we have

$$\int p(\boldsymbol{y},\boldsymbol{c}|\boldsymbol{\theta},\boldsymbol{s})d\boldsymbol{c} = p(y_1)\prod_{t=2}^{T}p(y_t|\mathcal{F}_{t-1})p(v_1;F_1)\prod_{t=2}^{T}p(v_t(s_{1:t-1});F_t(s_{1:t-1})),$$

where $\mathcal{F}_t$ denotes the information set up to t (*i.e.*, the natural filtration generated by $\{s_{1:t},\epsilon_{1:t},\eta_{1:t}\}$), such that $s_{1:t-1} = \{s_1,...,s_{t-1}\}$, and v_t is the (conditionally) independent

prediction error $y_t - E_{t-1}(\tau_t + c_t)$ with variance F_t obtained from the Kalman filter such that $v_t \sim N(0, F_t)$ for all t. Notice that v_1 and F_1 do not include s_t as s_1 only appears at $t = 2$ via the effect of c_2 on τ_1. This means that an unbiased estimator of the integrated likelihood (used to compute the log Bayes factor in the main text) is given by

$$\hat{p}(\boldsymbol{y}) = \frac{p(v_1; F_1)}{M} \sum_{i=1}^{M} \prod_{t=2}^{T-1} p(v_t(s_{1:t-1}^{(i)}); F_t(s_{1:t-1}^{(i)})),$$

where $s_{1:t-1}^{(i)}$, $i = 1, ..., M$, are drawn from $p(\boldsymbol{s})$ (*i.e.*, the bootstrap particle filter; see, *e.g.*, Doucet et al., 2001). This factorization is essentially a Rao-Blackwellization step that reduces the high-dimensional integral by the Kalman filter, a technique called mixture Kalman filter by Chen and Liu (2000) used in a class of martingale unobserved components models (Shephard, 2015)—more examples can be found in Li and Mendieta-Muñoz (2020) and Li and Koopman (2021).

By pointing out that $p(\boldsymbol{s}) = p(s_1) \prod_{t=2}^{T-1} p(s_t|s_{t-1})$, the evaluation of $\hat{p}(\boldsymbol{y})$ can be done sequentially via sequential Monte Carlo methods (Doucet et al., 2001). Usually, $p(s_t|s_{t-1})$ is replaced by some proposal density for efficiency, but considering that s_t is only binary, we adopt the simplest method by using $p(s_t|st-1)$ directly.

First, we set up the conditional state space representation of the H^{m}CUC model:

$$\begin{aligned} y_t &= \boldsymbol{Z}\boldsymbol{\alpha}_t, \\ \boldsymbol{\alpha}_t &= \boldsymbol{T}(s_{1:t-1})\boldsymbol{\alpha}_{t-1} + \boldsymbol{R}\boldsymbol{\zeta}_t, \quad \boldsymbol{\zeta} \sim N(\boldsymbol{0}, \boldsymbol{\Sigma}), \end{aligned}$$

where $\boldsymbol{\zeta}_t = (\eta_t, \epsilon_t)'$ and $\boldsymbol{\Sigma}$ are defined by equation (4) in the main text; and $\boldsymbol{\alpha}_t$ collects the trend and cycle whose transition dynamics is determined by $\boldsymbol{T}(s_{1:t-1})$, a predetermined matrix given

$s_{1:t-1}$. Specifically, we have

$$\boldsymbol{T}(s_{1:t-1}) = \begin{bmatrix} 1 & 0 & 0 & 0 & 0 & 0 & \dots & 0 \\ \mu_1 \mathbb{1}_{\{t<t_0\}} + \mu_2 \mathbb{1}_{\{t \geq t_0\}} & 1 & \beta_1 s_{t-1} & \beta_2 s_{t-2} & \beta_3 s_{t-3} & \beta_4 s_{t-4} & \dots & \beta_k s_{t-k} \\ 0 & 0 & \phi_1 & \phi_2 & 0 & 0 & \dots & 0 \\ 0 & 0 & 1 & 0 & 0 & 0 & \dots & 0 \\ 0 & 0 & 0 & 1 & 0 & 0 & \dots & 0 \\ 0 & 0 & 0 & 0 & 1 & 0 & \dots & 0 \\ \vdots & \vdots & \vdots & \vdots & \vdots & \ddots & \vdots & \vdots \\ 0 & 0 & 0 & 0 & 0 & \dots & 1 & 0 \end{bmatrix},$$

and $\boldsymbol{\alpha}_t$, $\boldsymbol{R}$, and $\boldsymbol{Z}$ are given by

$$\boldsymbol{\alpha}_t = \begin{bmatrix} 1 \\ \tau_t \\ c_t \\ c_{t-1} \\ c_{t-2} \\ c_{t-3} \\ \vdots \\ c_{t-k+1} \end{bmatrix}, \quad \boldsymbol{R} = \begin{bmatrix} 0 & 0 \\ 1 & 0 \\ 0 & 1 \\ 0 & 0 \\ 0 & 0 \\ 0 & 0 \\ \vdots & \vdots \\ 0 & 0 \end{bmatrix}, \quad \boldsymbol{Z}' = \begin{bmatrix} 0 \\ 1 \\ 1 \\ 0 \\ 0 \\ 0 \\ \vdots \\ 0 \end{bmatrix}.$$

Second, the algorithm for computing (the unbiased estimate of) the integrated likelihood is shown below:

1. At $t = 1$, let $\boldsymbol{a}_1 = (1, \tau_0 + \mu_1, \boldsymbol{0}_{1\times k})'$ and $\boldsymbol{P}_1 = \boldsymbol{R}\boldsymbol{\Sigma}\boldsymbol{R}'$.
   - Sample $\bar{\boldsymbol{\alpha}}_1^{(i)} \sim N(\boldsymbol{a}_1, \boldsymbol{P}_1)$, $i = 1, ..., M$. This is the same as considering $(\tau_1^{(i)}, c_1^{(i)})' \sim N((\tau_0 + \mu_1, 0)', \boldsymbol{\Sigma})$ and setting all pre-sample cycles to zero.
   - Compute the prediction error and associated variance matrix for $i = 1, ..., M$:

$$v_1^{(i)} = y_1 - \boldsymbol{Z}\bar{\boldsymbol{\alpha}}_1^{(i)},$$
$$F_1^{(i)} = \boldsymbol{Z}\boldsymbol{P}_1\boldsymbol{Z}'.$$

– Record the likelihood contribution for $i = 1, ..., M$, and their mean and variance:

$$w_1^{(i)} = \frac{1}{\sqrt{2\pi F_1^{(i)}}} \exp\left(-\frac{(v_1^{(i)})^2}{F_1^{(i)}}\right), \quad \hat{w}_1 = \frac{1}{M}\sum_{i=1}^{M} w_1^{(i)}, \quad \hat{s}_{w_1}^2 = \frac{1}{M-1}\sum_{i=1}^{M}(w_1^{(i)} - \hat{w}_1)^2.$$

– Estimate the log-likelihood contribution with bias correction (see Li and Koopman, 2021 for an explanation):

$$\hat{l}_1 = \log \hat{p}(y_1) = \log \hat{w}_1 + \frac{\hat{s}_{w_1}^2}{2M\hat{w}_1^2}.$$

– Normalize the likelihood contribution for $i = 1, ..., M$:

$$W_1^{(i)} = \frac{w_1^{(i)}}{\sum_{i=1}^{M} w_1^{(i)}}.$$

2. At $t = 2$, sample M particles:

$$s_1^{(i)} \sim Ber(1 - \bar{q}_0), \quad i = 1, ..., M.$$

Form $\boldsymbol{T}(s_1^{(i)})$ for $i = 1, ..., M$. Run the Kalman update.

– Compute the Kalman gain:

$$\boldsymbol{K}_1^{(i)} = \frac{\boldsymbol{T}(s_1^{(i)})\boldsymbol{P}_1\boldsymbol{Z}'}{F_1^{(i)}}.$$

– Compute the Kalman filter:

$$\begin{aligned}
\bar{\boldsymbol{\alpha}}_2^{(i)} &= \boldsymbol{T}(s_1^{(i)})\bar{\boldsymbol{\alpha}}_1^{(i)} + \boldsymbol{K}_1^{(i)} v_1^{(i)}, \\
\boldsymbol{P}_2^{(i)} &= \boldsymbol{T}(s_1^{(i)})\boldsymbol{P}_1(\boldsymbol{T}(s_1^{(i)}) - \boldsymbol{K}_1^{(i)}\boldsymbol{Z})'\boldsymbol{R}\boldsymbol{\Sigma}\boldsymbol{R}', \\
v_2^{(i)} &= y_2 - \boldsymbol{Z}\bar{\boldsymbol{\alpha}}_2^{(i)}, \\
F_2^{(i)} &= \boldsymbol{Z}\boldsymbol{P}_2^{(i)}\boldsymbol{Z}'.
\end{aligned}$$

– Record the likelihood contribution for $i = 1, ..., M$, and their mean and variance:

$$w_2^{(i)} = W_1^{(i)} \frac{1}{\sqrt{2\pi F_2^{(i)}}} \exp\left(-\frac{(v_2^{(i)})^2}{F_2^{(i)}}\right), \quad \hat{w}_2 = \frac{1}{M}\sum_{i=1}^{M} w_2^{(i)}, \quad \hat{s}_{w_2}^2 = \frac{1}{M-1}\sum_{i=1}^{M}(w_2^{(i)} - \hat{w}_2)^2.$$

– Estimate the log-likelihood contribution with bias correction:

$$\hat{l}_2 = \log \hat{p}(y_2|\mathcal{F}_1) = \log \hat{w}_2 + \frac{\hat{s}_{w_2}^2}{2M\hat{w}_2^2}.$$

– Normalize the likelihood contribution for $i = 1, ..., M$:

$$W_2^{(i)} = \frac{w_2^{(i)}}{\sum_{i=1}^{M} w_2^{(i)}}.$$

– Compute the particle ESS:

$$\Gamma_2 = \frac{1}{\sum (W_2^{(i)})^2}.$$

– If $\Gamma_2 < 0.75M$, resample with replacement M particles (see Doucet et al., 2001 for generic treatments of resampling in particle filters):

$$\{s_1^{(i)}, \boldsymbol{T}(s_1^{(i)}), \bar{\boldsymbol{\alpha}}_2^{(i)}, \boldsymbol{P}_2^{(i)}, v_2^{(i)}, F_2^{(i)}\} \propto W_2^{(i)},$$

and set $W_2^{(i)} = 1/M$.

3. At $t \geq 3$, sample M particles:

$$s_{t-1}^{(i)} \sim P(s_{t-1}^{(i)}|s_{t-2}^{(i)}), \quad i = 1, ..., M.$$

Form $\boldsymbol{T}(s_{1:t-1}^{(i)})$ for $i = 1, ..., M$. Run the Kalman update.

– Compute the Kalman gain:

$$\boldsymbol{K}_{t-1}^{(i)} = \frac{\boldsymbol{T}(s_{1:t-1}^{(i)})\boldsymbol{P}_{t-1}^{(i)}\boldsymbol{Z}'}{F_{t-1}^{(i)}}.$$

– Compute the Kalman filter:

$$\begin{aligned}
\bar{\boldsymbol{\alpha}}_t^{(i)} &= \boldsymbol{T}(s_{1:t-1}^{(i)})\bar{\boldsymbol{\alpha}}_{t-1}^{(i)} + \boldsymbol{K}_{t-1}^{(i)} v_{t-1}^{(i)}, \\
\boldsymbol{P}_t^{(i)} &= T(s_{1:t-1}^{(i)}) P_1 (T(s_{1:t-1}^{(i)}) - \boldsymbol{K}_{t-1}^{(i)} \boldsymbol{Z})' \boldsymbol{R}\boldsymbol{\Sigma}\boldsymbol{R}', \\
v_t^{(i)} &= y_t - \boldsymbol{Z}\bar{\boldsymbol{\alpha}}_t^{(i)}, \\
F_t^{(i)} &= \boldsymbol{Z}\boldsymbol{P}_t^{(i)}\boldsymbol{Z}'.
\end{aligned}$$

– Record the likelihood contribution for $i = 1, ..., M$, and their mean and variance:

$$w_t^{(i)} = W_{t-1}^{(i)} \frac{1}{\sqrt{2\pi F_t^{(i)}}} \exp\left(-\frac{(v_t^{(i)})^2}{F_t^{(i)}}\right), \;\; \hat{w}_t = \frac{1}{M}\sum_{i=1}^{M} w_t^{(i)}, \;\; \hat{s}_{w_t}^2 = \frac{1}{M-1}\sum_{i=1}^{M}(w_t^{(i)} - \hat{w}_t)^2.$$

– Estimate the log-likelihood contribution with bias correction:

$$\hat{l}_t = \log \hat{p}(y_t|\mathcal{F}_{t-1}) = \log \hat{w}_t + \frac{\hat{s}_{w_t}^2}{2M\hat{w}_t^2}.$$

– Normalize the likelihood contribution for $i = 1, ..., M$:

$$W_t^{(i)} = \frac{w_t^{(i)}}{\sum_{i=1}^{M} w_t^{(i)}}.$$

– Compute the particle ESS:

$$\Gamma_t = \frac{1}{\sum (W_t^{(i)})^2}.$$

– If $\Gamma_t < 0.75M$, resample with replacement M particles:

$$\{s_{t-1}^i, T(s_{t-1}^{(i)}), \bar{\boldsymbol{\alpha}}_t^{(i)}, \boldsymbol{P}_t^{(i)}, v_t^{(i)}, F_t^{(i)}\} \propto W_t^{(i)},$$

and set $W_t^{(i)} = 1/M$.

4. The total log-likelihood is given by

$$\log \hat{p}(\boldsymbol{y}) = \sum_{t=1}^{T} \hat{l}_t.$$

This is then used for computing the log Bayes factor for model comparison and Bayesian averaging, as discussed in the main text. In our implementation, we set $M = 10,000$. We also point out that, due to the discrete state values that the latent Markov process s_t can assume, resampling occurs rarely, which is evidence in favor of an efficient sequential Monte Carlo algorithm.

References

Basistha, A. (2007). Trend-cycle correlation, drift break and the estimation of trend and cycle in Canadian GDP. *Canadian Journal of Economics/Revue canadienne d'économique 40*(2), 584–606.

Benati, L. and T. A. Lubik (2022). Searching for hysteresis. *Federal Reserve Bank of Richmond Working Paper*, 22–05.

Chen, R. and J. S. Liu (2000). Mixture Kalman filters. *Journal of the Royal Statistical Society: Series B (Statistical Methodology) 62*(3), 493–508.

Chib, S. and E. Greenberg (1995). Understanding the Metropolis-Hastings algorithm. *The american statistician 49*(4), 327–335.

Doucet, A., N. De Freitas, N. J. Gordon, et al. (2001). *Sequential Monte Carlo methods in practice*, Volume 1. Springer.

Furlanetto, F., A. Lepetit, Ø. Robstad, J. Rubio Ramírez, and P. Ulvedal (2021). Estimating hysteresis effects. *CEPR Discussion Paper*, No. DP16558.

González-Astudillo, M. and J. M. Roberts (2022). When are trend–cycle decompositions of GDP reliable? *Empirical Economics 62*(5), 2417–2460.

Grant, A. L. and J. C. Chan (2017). A Bayesian model comparison for trend-cycle decompositions of output. *Journal of Money, Credit and Banking 49*(2-3), 525–552.

Kim, C.-J. (1994). Dynamic linear models with Markov-switching. *Journal of econometrics 60*(1-2), 1–22.

Li, M. and S. J. Koopman (2021). Unobserved components with stochastic volatility: Simulation-based estimation and signal extraction. *Journal of Applied Econometrics 36*(5), 614–627.

Li, M. and I. Mendieta-Muñoz (2020). Are long-run output growth rates falling? *Metroeconomica 71*(1), 204–234.

Li, M. and I. Mendieta-Muñoz (2021). Bayesian analysis of structural correlated unobserved components and identification via heteroskedasticity. *Studies in Nonlinear Dynamics & Econometrics 26*(3), 337–359.

Morley, J. C., C. R. Nelson, and E. Zivot (2003). Why are the Beveridge-Nelson and unobserved-components decompositions of GDP so different? *Review of Economics and Statistics 85*(2), 235–243.

Oh, K. H., E. Zivot, and D. Creal (2008). The relationship between the Beveridge–Nelson decomposition and other permanent–transitory decompositions that are popular in economics. *Journal of Econometrics 146*(2), 207–219.

Shephard, N. (2015). Martingale unobserved component models. In S. J. Koopman and N. Shephard (Eds.), *Unobserved Components and Time Series Econometrics*, pp. Chapter 10. Oxford University Press.

Stock, J. H. and M. W. Watson (1998). Median unbiased estimation of coefficient variance in a time-varying parameter model. *Journal of the American Statistical Association 93*(441), 349–358.

Trenkler, C. and E. Weber (2016). On the identification of multivariate correlated unobserved components models. *Economics Letters 138*, 15–18.